Bioorganic Chemistry 92 (2019) 103271

Contents lists available at ScienceDirect

Bioorganic Chemistry

journal homepage: www.elsevier.com/locate/bioorg

Synthesis and biological evaluation of thiazolidine-2,4-dione-pyrazole conjugates as antidiabetic, anti-inflammatory and antioxidant agents

Garima Bansal[a], Shamsher Singh[b], Vikramdeep Monga[a], Punniyakoti Veeraveedu Thanikachalam[a,*], Pooja Chawla[a,*]

[a] Department of Pharmaceutical Chemistry, ISF College of Pharmacy, Moga 142001, Punjab, India
[b] Department of Pharmacology, ISF College of Pharmacy, Moga 142001, Punjab, India

ARTICLE INFO

Keywords:
Thiazolidine-2,4-dione
PPAR-γ
Alpha amylase
Antidiabetic
Anti-inflammatory
Antioxidant

ABSTRACT

A series of fourteen novel thiazolidine-2,4-dione derivatives clubbed with pyrazole moiety were synthesized via four step reaction procedure. Reactions were monitored by thin layer chromatography and were characterized by physicochemical and spectrophotometric (IR, Mass, ^{1}HNMR and ^{13}CNMR) analysis. The spectral data were in good agreement with their structures. The title compounds were docked against peroxisome proliferated activated receptors (PPAR-γ) and alpha-amylase and further evaluated for *in vivo* and *in vitro* antidiabetic, *in vitro* anti-inflammatory and antioxidant activities. Compound **GB14** exhibited significant blood glucose lowering activity and was also found to be active inhibitor of alpha-amylase. Compound **GB7** was found to be potent anti-inflammatory agent in terms of reducing inflammatory markers (TNF-α, IL-β, MDA) and also showed antioxidant activity to good extent. Therefore, these compounds may be considered as promising candidates for the development of new antidiabetic agents.

1. Introduction

Diabetes is an unceasing, metabolic disease characterized by elevated levels of blood glucose (or blood sugar), which over a period of time leads to serious damage to the heart, blood vessels, eyes, kidneys, and nerves. India currently represents 49 percent of the world's diabetes burden, with an estimated 72 million cases in 2017, a figure expected to almost double to 134 million by 2025 [1]. Being classified as type 1, type 2 and gestational diabetes, Type 2 diabetes mellitus is the common major form of diabetes which is the consequence of defect(s) in insulin secretion, mainly with a major contribution from insulin resistance [2].

Thiazolidine-2,4-dione (TZD), a potent agonist of peroxisome proliferated activated receptor (PPAR-γ) activates it thereby, altering the transcription of several genes involved in glucose and lipid metabolism and also energy balance [3]. As reported, diabetes is associated with various complications, among which diabetic nephropathy is one of the most frequent microvascular complication [4]. Both inflammation and oxidative stress are closely associated with the progress of diabetic nephropathy (Fig. 1) [5,6]. Increase in oxidative stress can increase the production of inflammatory cytokines and likewise, an increase in inflammatory cytokines can stimulate the production of free radicals [7]. Therefore, drugs with anti-inflammatory properties such as TZDs (clubbed with pyrazole) can probably reduce the risk of developing diabetes and diabetes-induced problems. TZDs inhibit the expression of a variety of proteins with proinflammatory properties, including cyclooxygenase-2 (COX-2), inducible nitric-oxide synthase (iNOS), and several cytokines [8]. However, the molecular mechanisms responsible for these activities have not yet been clarified.

Several studies have shown that diabetes mellitus is accompanied by augmented development of free radicals (reactive oxygen species) and decreased antioxidant capacity (reduced free radical scavenging activity and increased plasma oxidisability), leading to oxidative damage of cell components [9–11]. When the balance between free radicals formation and their detoxification is disrupted, which is necessary for normal functioning of the cell, a cell enters a state of oxidative stress and is damaged [12]. As reported, TZDs considerably augmented the expression of glutathione peroxidase 3 (GPx3), and the antioxidative result of PPAR-γ was caused primarily by GPx3 in myotubes [13]. There are many proven studies reporting that TZDs conserve islet β -cell function in patients with diabetes or high risk for diabetes [14]. In addition, TZDs progress islet β-cell function and diminish the oxidative stress in islets of *db/db* mice [15]. Even though the expression level of PPAR-γ is pretty low in islets, numerous reports have shown protective

* Corresponding authors.
E-mail addresses: nspkoti2001@gmail.com (P.V. Thanikachalam), pvchawla@gmail.com (P. Chawla).

https://doi.org/10.1016/j.bioorg.2019.103271
Received 9 June 2019; Received in revised form 2 September 2019; Accepted 9 September 2019
Available online 10 September 2019
0045-2068/

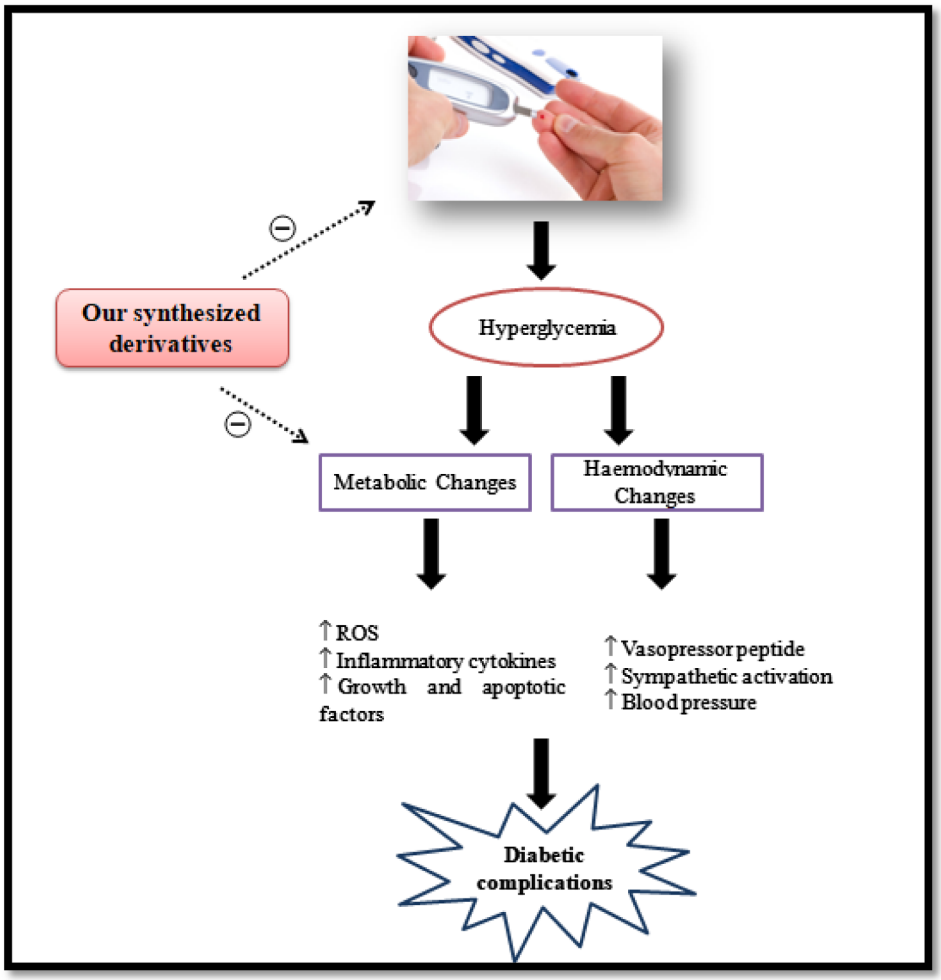

Fig. 1. Targets of synthesized derivatives.

effects of TZDs against glucose- or lipid-induced toxicity in islets [16]. These reports proposed that TZDs unswervingly provide positive effects on islet β-cells, and the reduction of oxidative stress may play a vital role in this process. As there are some side effects linked with TZDs like weight gain, edema, hepatotoxicity, TZDs might be discovered as antidiabetics including alpha-amylase inhibitors and may reduce the glucose levels that can occur after a meal by slowing the speed of conversion of starch to monosaccharides [17,18].

Derivatization of existing molecules is one of the most resourceful strategies in the designing of drug and is based on the clubbing of pharmacophoric scaffolds of different bioactive compounds to fabricate a new fused compound with enhanced affinity and efficiency when compared to the parent molecules. Guided by the above information and in continuation of our previous work done on TZD moiety, we have designed pioglitazone/celecoxib hybrids (Fig. 2) containing thiazolidindione core as central ring (diabetic scaffold) bearing diaryl pyrazole moiety (anti-inflammatory scaffold) to discover new candidates thereby, possessing anti-diabetic, anti-inflammatory and antioxidant activities [19,20].

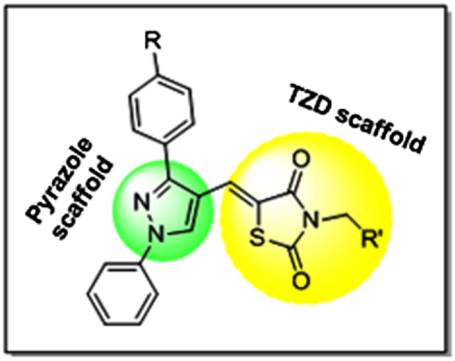

Fig. 2. Designed molecular hybrid.

2. Results and discussion

2.1. Chemistry

The proposed compounds (**GB1-GB14**) were synthesized using a synthetic procedure involving 4 steps and the synthetic strategy is outlined in Scheme 1. Thiourea on refluxing with chloroacetic acid gives thiazoldine-2,4-dione [21]. Hydrazones were synthesized by treating substituted acetophenones with phenyl hydrazine followed by Vilsmeier-Haack reaction in the presence of DMF and $POCl_3$ to give pyrazole carbldehydes [22]. *N*-allylation and acidification of TZD was carried out with benzyl bromide and bromoacetic acid, respectively followed by Knoevenagel condensation with synthesized carbaldehydes to yield TZD clubbed pyrazole adducts (GB1-GB14) [23–25]. All new compounds were characterized by physico-chemical, IR (Shimadzu 8400 S), ^{1}HNMR, ^{13}CNMR (Bruker Avance II 400 MHz) and mass spectrometry (Shimadzu QP2010 ULTRA GC–MS). The spectral data were in good agreement with their structures. The IR values are expressed in cm^{-1} and the chemical shifts are reported in parts per

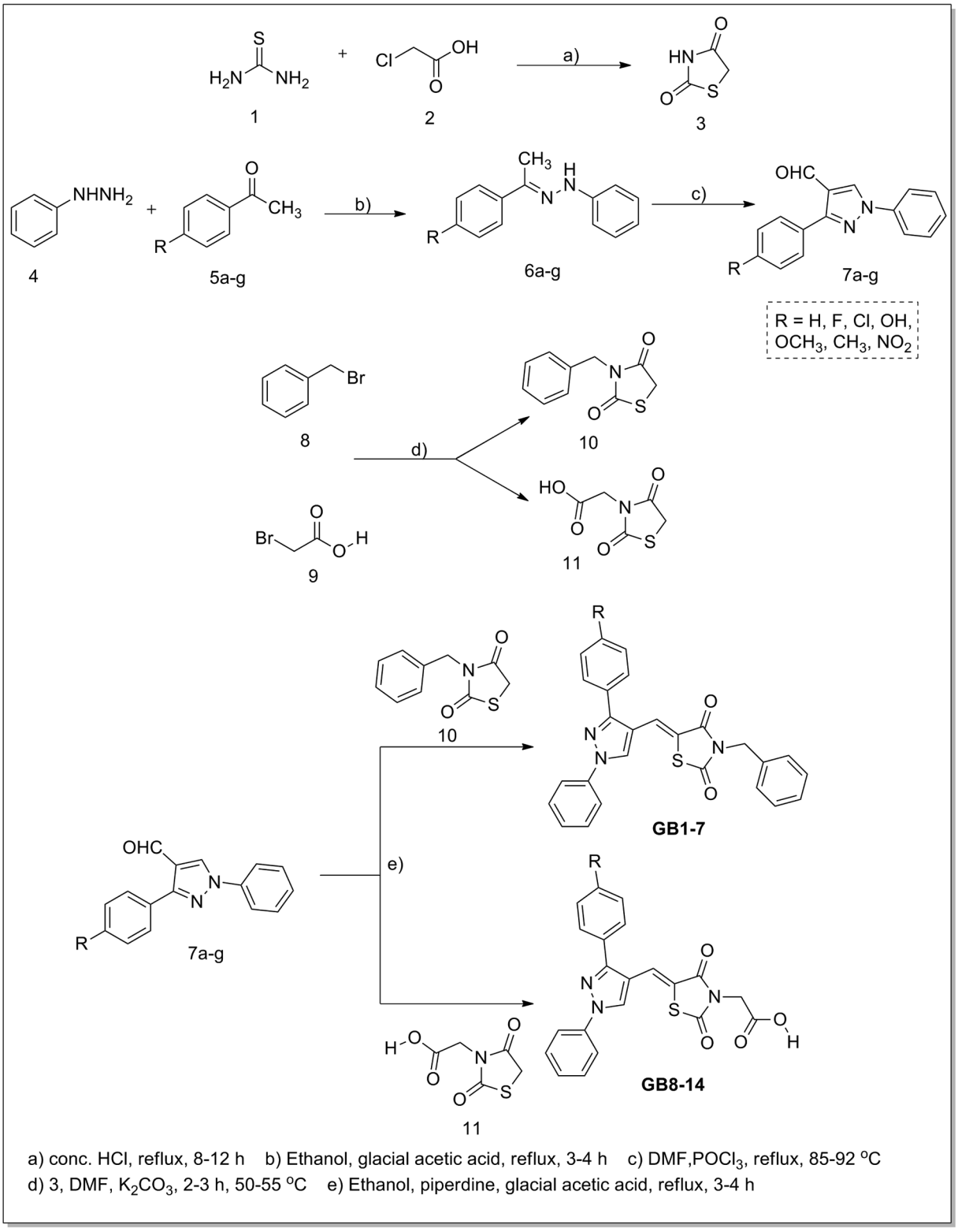

Scheme 1. Synthesis of TZD clubbed pyrazoles (GB1-GB14).

million (δ value) from TMS (δ 0 ppm for ^{1}H NMR) as an internal standard. Coupling constant are given in Hertz. The structure of final derivatives is shown in Fig. 3.

2.2. Molecular docking studies

Molecular docking was carried out to investigate some possible structural insights into the potential binding patterns of the synthesized molecules GB1-GB14 with the active sites of target PPARγ (PDB ID: 2PRG) and α-amylase (PDB ID: 4GQR) using MOE software. The various possible interactions and orientations were investigated and compared with the binding patterns of pioglitazone and acarbose for both anti-diabetic and α-amylase activity. In interaction with PPAR-γ, compounds **GB8**, **GB11** and **GB14** displayed best docking scores with values

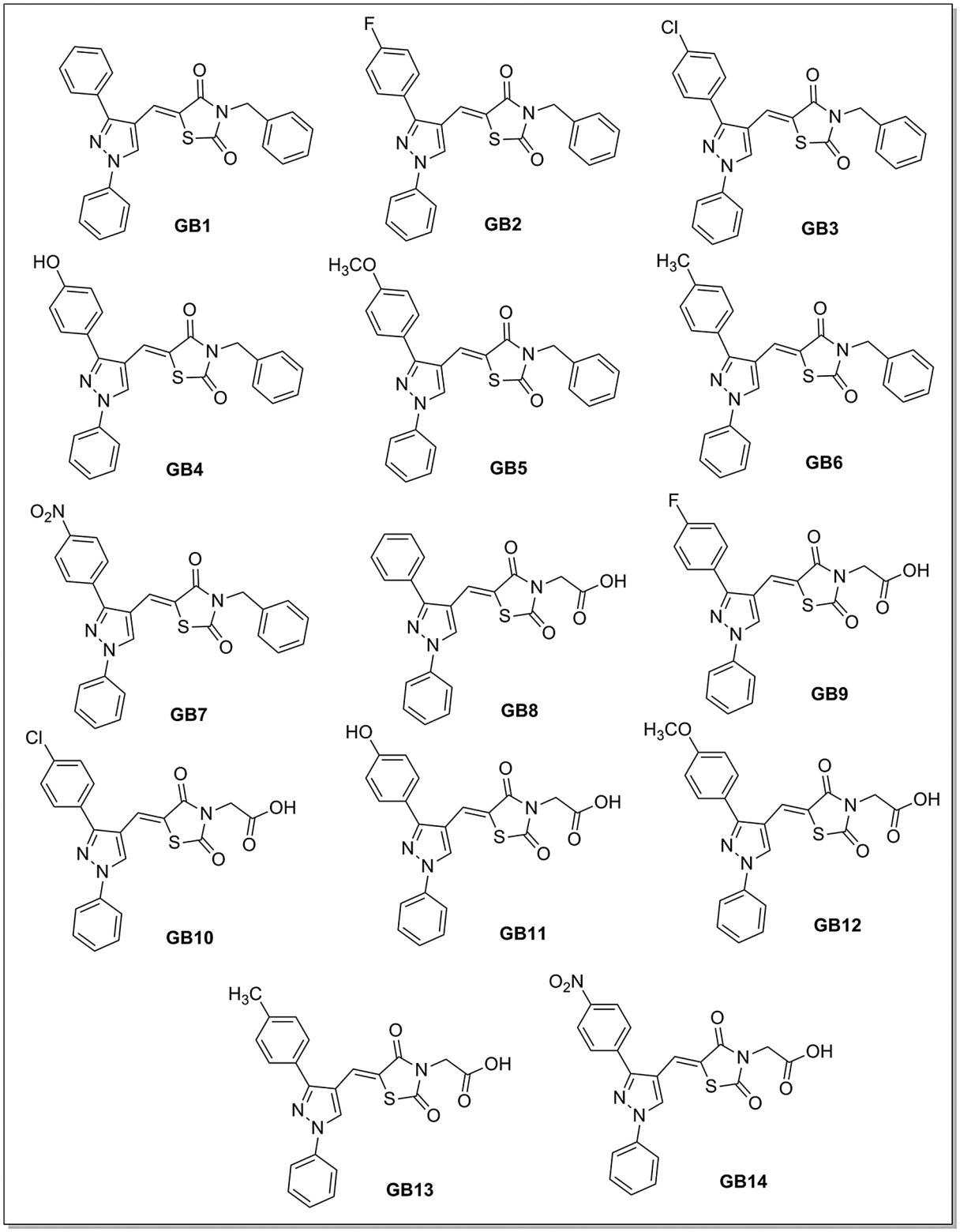

Fig. 3. Structures of final derivatives.

of −15.13, −16.79 and −17.44 which were better than the reference drug pioglitazone (-12.605). Compound **GB8** showed four hydrogen bond interactions, one keto group with water molecule in association to Arg A288, another keto group with amino acid residues Ser A342 (2.86 Å) and with water molecule in association with Ser A342 and acidic hydroxyl group interaction with water molecule in association with Ser A342 (Fig. 4). The hydroxyl group of compound **GB11** showed hydrogen bonding interaction with water in association to Glu A272; whereas other hydrogen bonding interaction with Glu A272 (1.25 Å) and also with Gln A271 (2.78 Å) (Fig. 5). Compound **GB14** showed only one interaction through water molecule in association with Gly A284 as depicted in Fig. 6. The acidic head of pioglitazone (NH and carbonyl) showed interaction with water molecule associated with Arg A288 as shown in Fig. 7. In interaction with α-amylase, compounds **GB11**,

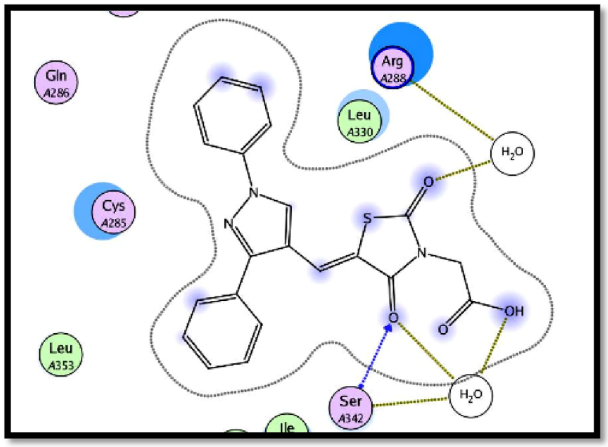

(a)

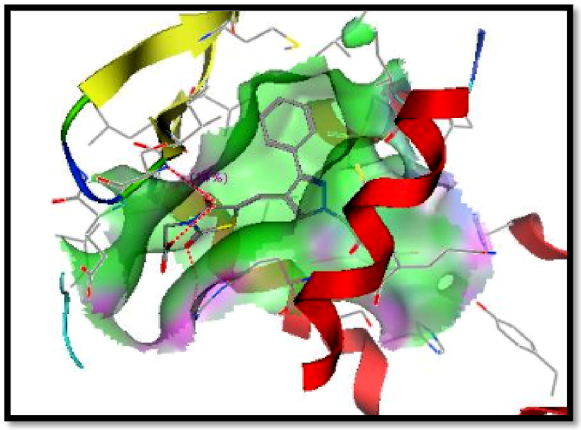

(b)

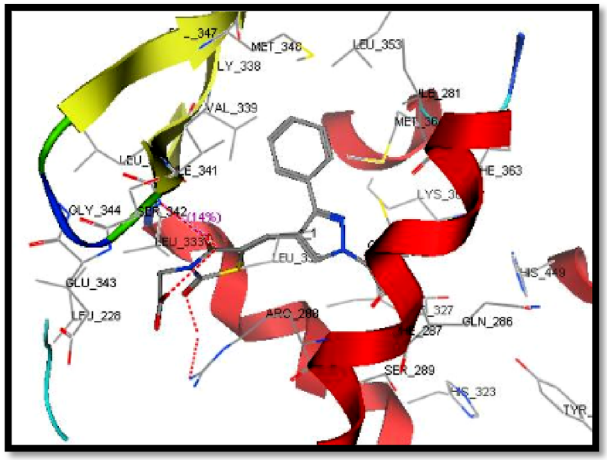

(c)

Fig. 4. (a) 2D interactions of GB8 with PPAR-γ (b) 3D pose of embedded ligand inside the pocket (c) Possible interactions between ligand and receptor.

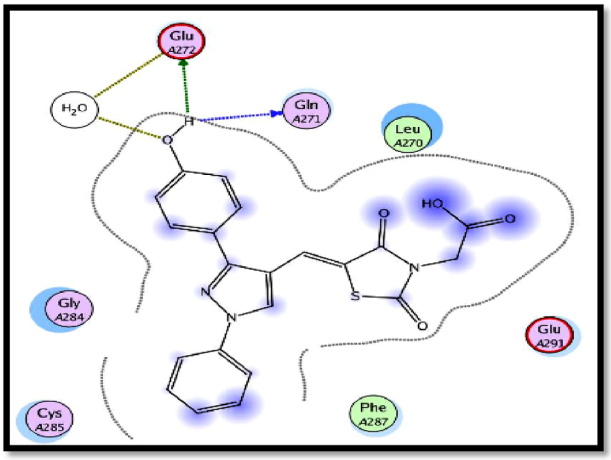

(a)

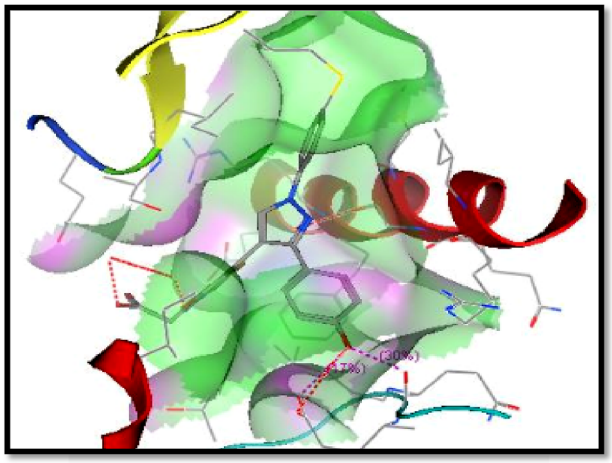

(b)

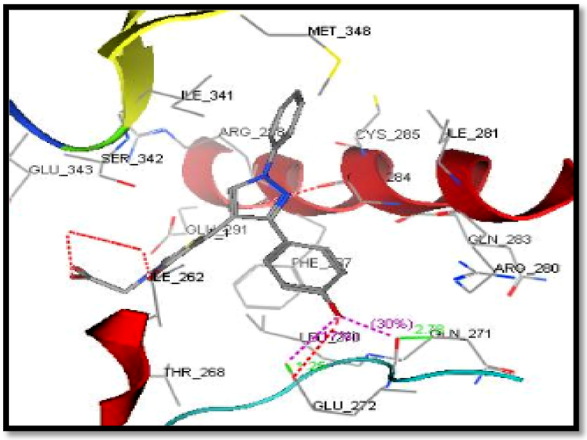

(c)

Fig. 5. (a) 2D interactions of GB11 with PPAR-γ (b) 3D pose of embedded ligand inside the pocket (c) Possible interactions between ligand and receptor.

GB12 and **GB14** displayed best docking scores with values of −16.63, −17.59 and −17.98 whereas the reference drug acarbose showed docking score with value of −26.33. Compound GB-11 showed two interactions, one hydroxyl group with water molecule in association to Arg 195, and another pi-pi interaction with amino acid residues Trp 59 (4.76 Å) (Fig. 8). The acidic carbonyl group of compound GB-12 showed solvent interaction (H_2O) in association with Glu 233, Asn 298, Ala 307 and Asp 300 (Fig. 9). The carbonyl acidic group of compound **GB14** showed two hydrogen bonding interaction with water in association to Ala 307 and Asp 300 and one in direct contact with Asp 300, compound also showed pi-pi interaction with phenyl ring of Trp 59 (Fig. 10). The standard acarbose showed many interactions with water molecule associated with Ala 307, Asp 300, Glu 233, Asn 298, Thr 163 and Arg 195. The hydroxyl group also showed interactions with Ala 307, Thr 163 and Asp 300 as shown in Fig. 11. From the findings, it is evident that the pattern of binding in the active site of PPAR-γ and α-amylase is almost similar to that of pioglitazone and

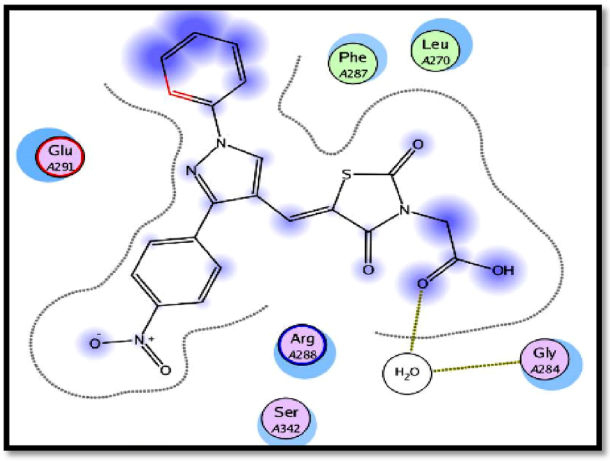

(a)

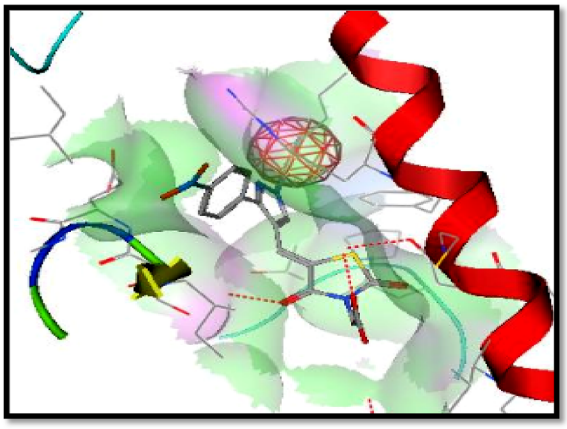

(b)

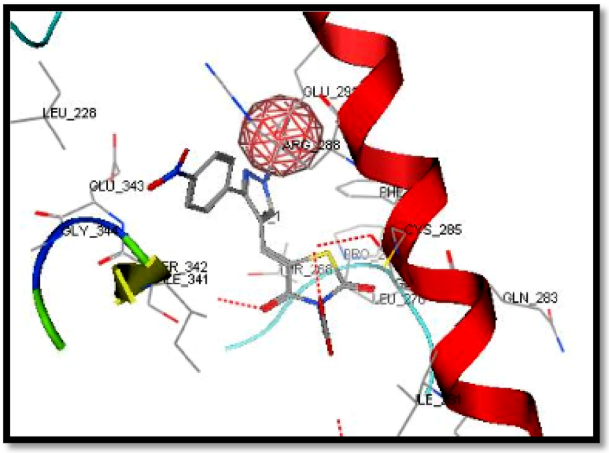

(c)

Fig. 6. (a) 2D interactions of GB14 with PPAR-γ (b) 3D pose of embedded ligand inside the pocket (c) Possible interactions between ligand and receptor.

acarbose which are well-established therapeutic candidates for diabetes.

2.3. Biological activity

The synthesized derivatives were subjected to pharmacological screening for antidiabetic activity against STZ-NA induced diabetes in mice, *in vitro* α-amylase activity, *in vitro* anti-inflammatory and antioxidant activity using DPPH method.

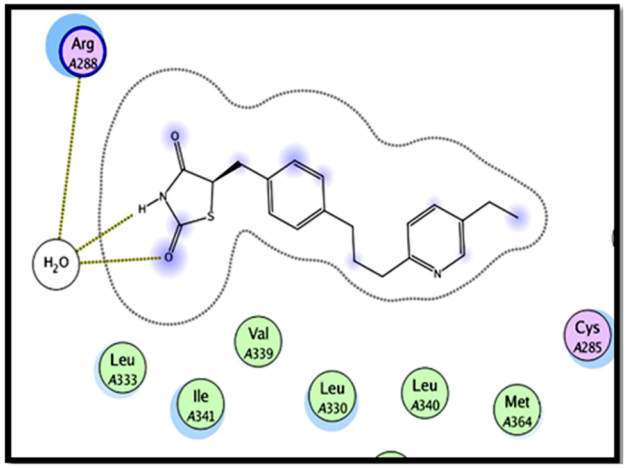

Fig. 7. 2D interactions of pioglitazone with PPAR-γ.

2.3.1. In vivo antidiabetic activity

From the docking results, three compounds **GB8**, **GB11** and **GB14** showed the best docking scores and were further evaluated for antidiabetic activity in C57BL/6J mice. After administration of a single dose of these compounds, the blood glucose levels were monitored as per standard protocols on 1st, 3rd, 7th and 14th day of the initiation of experiment. As per the analyzed data, compound GB-14 and GB-8 showed 134.46 ± 0.49 and 136.28 ± 0.79 blood glucose lowering effect as compared to standard pioglitazone (136.56 ± 0.64) whereas compound **GB11** showed moderate blood glucose lowering effect (139.22 ± 0.66) (Table 1). Therefore compound **GB-14** showed the most potent results which were found to be consistent with the docking results and might occurred due to the activation of PPAR-γ receptors (Fig. 12).

2.3.2. In vitro alpha-amylase inhibitory activity assay

All the synthesized compounds were tested for their α-amylase activity. It was observed that acidic derivatives (GB8-GB14) showed more potent α-amylase inhibitory action as compared to benzylated derivatives. Among acidic derivatives, it was observed that compounds **GB12** and **GB14** were found to be active inhibitors of α-amylase enzyme at different extents but better than acarbose (Table 2). Log concentrations versus percentage inhibition curves were plotted and IC_{50} values were calculated for all compounds (Fig. 13). Among these, **GB14** has shown the highest activity against α-amylase with IC_{50} 4.08 μg/mL whereas GB-12 was the second most potent α-amylase inhibitor with IC_{50} 7.59 μg/mL. Both of them were found better than acarbose which was having IC_{50} 8.0 μg/mL.

2.3.3. Anti-inflammatory activity

The *in vitro* anti-inflammatory studies evaluated the ability of the target derivatives GB1-GB14 to lower down the expression of inflammatory markers (TNF-α, IL-1β and MDA) using an enzyme immunoassay (EIA). The data (Tables 3–5) showed that the target compounds possessed significant anti-inflammatory activity when compared to control. Benzylated TZDs were shown to give more potent results than the acidic TZDs and also aming benzylated TZD, compound with nitro substitution (**GB7**) came out to be the most potent derivative. Then, comes the more potent compounds with electron releasing group (Cl or F) (Figs. 14–16). Among all, the best lowering inflammatory marker was found to be IL-1β.

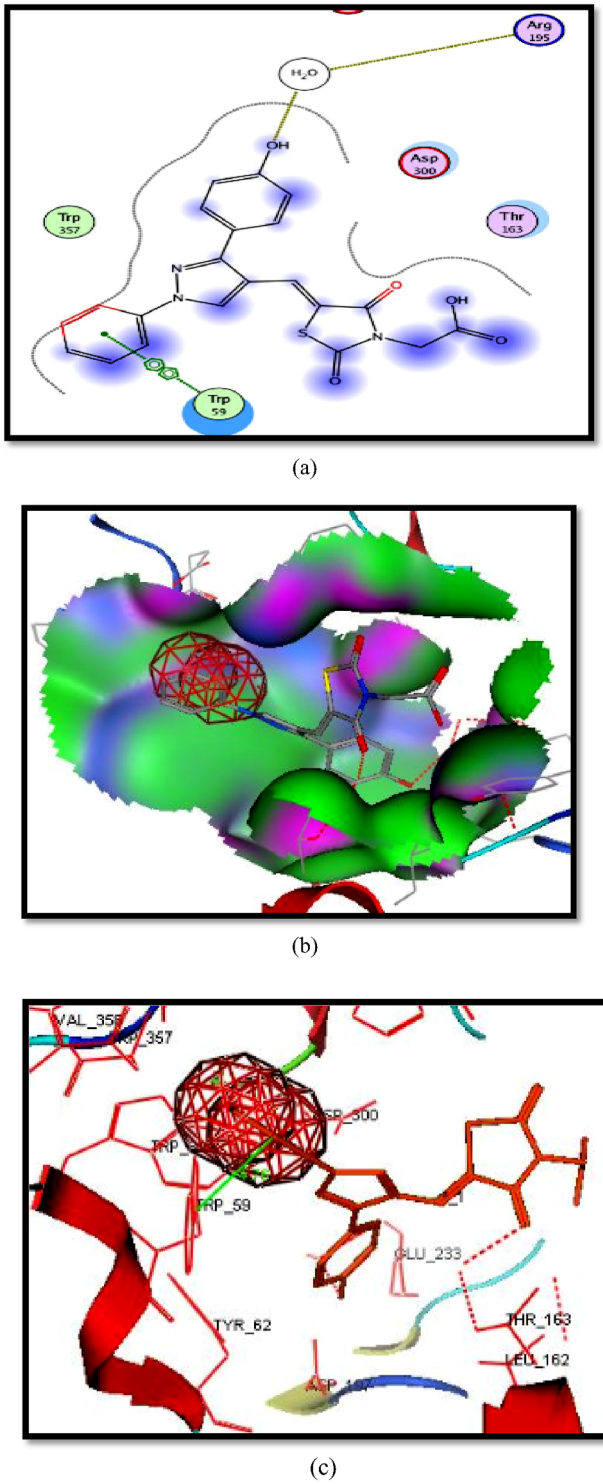

Fig. 8. (a) 2D interactions of GB11 with α-amylase (b) 3D pose of embedded ligand inside the pocket (c) Possible interactions between ligand and receptor.

2.3.4. Antioxidant activity

The synthesized compounds were evaluated for their *in vitro* antioxidant activity by DPPH method using ascorbic acid as standard. The results showed that all the synthesized compounds showed good antioxidant activity in comparison to ascorbic acid, wherein compounds **GB4**, **GB5** and **GB8** showed the most potent results with IC_{50} values of 110.88, 127.18 and 128.55 μg/mL, respectively. The standard drug ascorbic acid showed the IC_{50} value 81.12 μg/mL (Table 6 and Fig. 17).

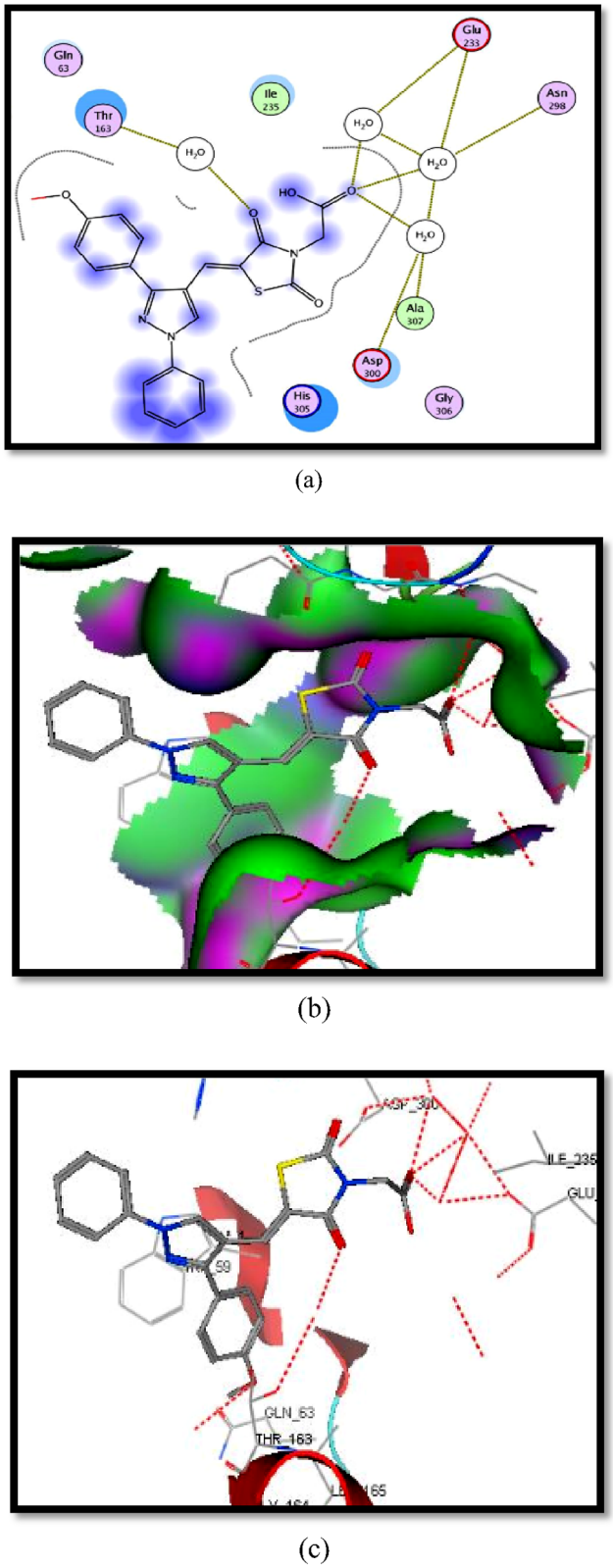

Fig. 9. (a) 2D interactions of GB12 with α-amylase (b) 3D pose of embedded ligand inside the pocket (c) Possible interactions between ligand and receptor.

Since all the three compounds (**GB4**, **GB5** and **GB8**) showed promising results potent analogues and therefore, can be used as novel lead molecule for future research work and these compounds might lead to the development of additional treatments directed towards the disorders caused by free radicals.

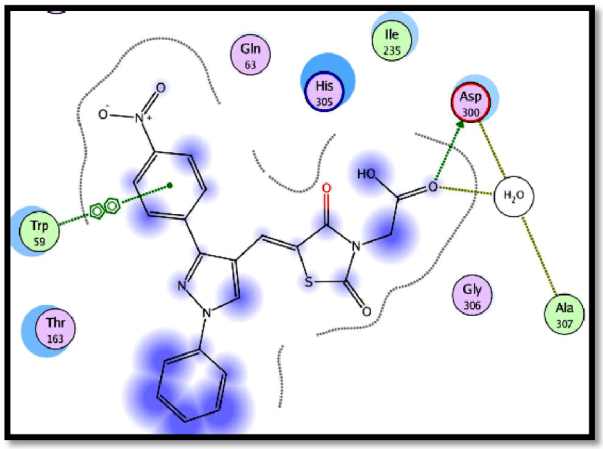

(a)

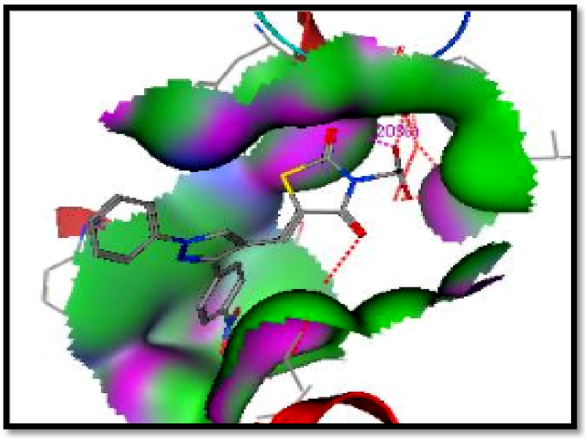

(b)

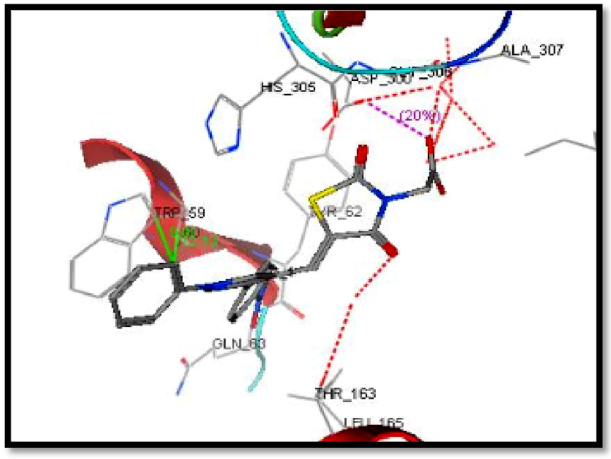

(c)

Fig. 10. (a) 2D interactions of GB14 with α-amylase (b) 3D pose of embedded ligand inside the pocket (c) Possible interactions between ligand and receptor.

2.4. Structure activity relationship (SAR)

As regards the relationship between the structures of the various synthesized scaffolds and the observed antidiabetic, anti-inflammatory and antioxidant activity, it showed varied biological activity. The SAR of the synthesized compounds are analysed on the basis of substitution on aryl ring attached to pyrazole core along with nature of *N*-substitution (TZD head). In case of antidiabetic activity, the acidic head

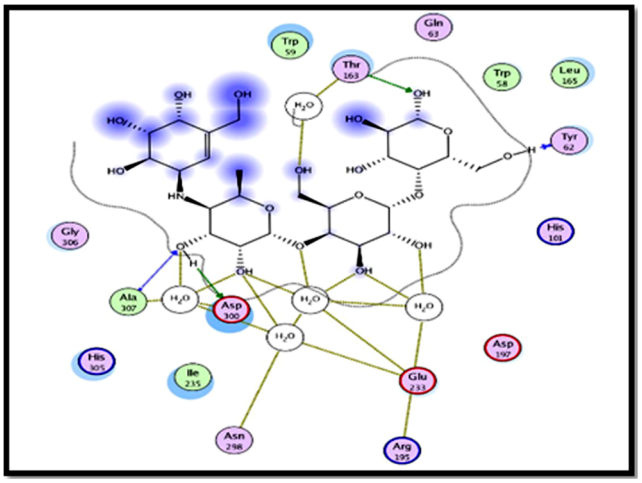

Fig. 11. 2D interactions of acarbose with α-amylase.

derivatives were found to be most potent in comparison to benzylated TZD along with electron withdrawing substitution on aryl ring of pyrazole (**GB14**). Compounds containing electron releasing groups further showed decreased activity (**GB2** and **GB3**). In case of anti-inflammatory activity, benzylated TZDs exhibited significant results and along with electron withdrawing group substitution on pyrazole ring (**GB7**). In case of antioxidant activity, the benzylated TZDs showed more potent results (**GB4** and **GB5**) rather than acidic TZDs.

3. Conclusion

A total of fourteen novel diaryl pyrazolyl thiazolidinediones were synthesized via Knoevenagel condensation of substituted pyrazole carboxaldehdyes with TZDs and along with *N*-substitution using benzyl bromide and bromoacetic acid, respectively. The resulting compounds were docked in order to study the ligand protein interactions of designed compounds with PPAR-γ (PDB ID-2PRG) and alpha-amylase (PDB ID-4GQR) using MOE software version 2008.10. Compounds **GB8**, **GB11** and **GB14** were well docked in the active site of PPAR-γ and compounds **GB11**, **GB12** and **GB14** were well docked in the active site of alpha-amylase with the best docking scores. The compounds with best docking scores were further screened for antidiabetic activity in STZ-induced diabetic mice. Compound **GB14** equipped with 4-nitro phenyl group along with acidic head showed significant blood glucose lowering effect (134.46 mg/dL) quite comparable to pioglitazone (136.56 mg/dL). Compounds **GB12** (IC_{50}: 7.59 μg/mL) and **GB14** (IC_{50}: 4.08 μg/mL) were found to be active inhibitors of alpha-amylase enzyme at different extents and also better than acarbose (IC_{50}: 8.0 μg/mL) on *in vitro* evaluation for alpha-amylase activity. The *in vitro* anti-inflammatory screening results showed that the benzylated TZDs along with NO_2 (**GB7**) exhibited the most potent results. Additionally, compounds were also evaluated for antioxidant activity by DPPH method. As a result, compounds (**GB4**, **GB5** and **GB8**) exhibited promising results and showed IC_{50} values of 110.88, 127.18 and 128.55 μg/mL, respectively and the results were compared to standard drug acarbose (81.12 μg/mL). The compounds with good activity profiling may be used as novel lead for future research work.

4. Experimental section

All the chemicals were purchased from CDH, Hi-Media, Loba Chemie and Sigma-Aldrich. Reactions were monitored by thin layer chromatography (TLC) on precoated silica-gel plates and visualized using ultraviolet light and iodine. Recrystallization of compounds was performed with chloroform-methanol and ethylacetate mixture. The melting points were determined by open capillary method and are

Table 1
Blood glucose levels of STZ-induced diabetic mice (*P < 0.001 when compared with diabetic control, n = 6).

Groups (n = 6)	Blood Glucose Level (mg/dL) ± S.D.			
	0 day	3rd day	7th day	14th day
Group I (Control)	112.28 ± 0.77	113.96 ± 0.52***	109.93 ± 0.51***	110.79 ± 0.77***
Group II (Diabetic control)	113.30 ± 0.45	264.08 ± 0.79	313.14 ± 0.77	387.88 ± 0.76
Group III (GB-8)	115.68 ± 0.53	288.54 ± 0.79***	185.45 ± 0.61***	136.28 ± 0.79***
Group IV (GB-11)	110.76 ± 0.64	267.48 ± 0.51	188.33 ± 0.88***	139.22 ± 0.66***
Group V (GB-14)	**115.44 ± 0.73**	**267.85 ± 0.59**	**189.44 ± 0.52*****	**134.46 ± 0.49*****
Group VI (Pioglitazone)	108.42 ± 0.74	250.40 ± 0.69***	184.90 ± 0.68***	136.56 ± 0.64***

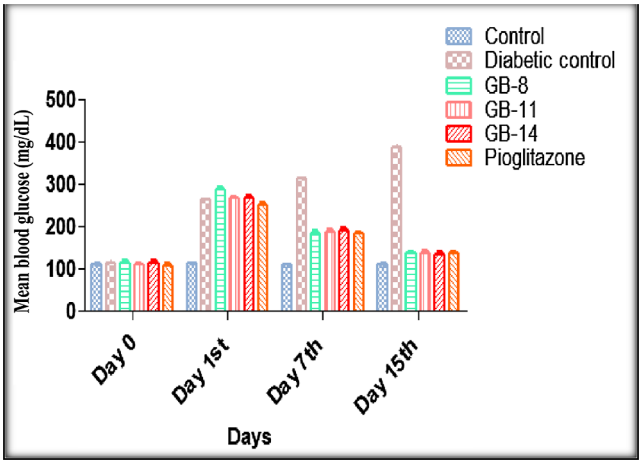

Fig. 12. Antidiabetic activity of compounds in STZ-induced diabetic rats. Data are analyzed by two-way ANOVA followed by Dunnett's *t*-test and expressed as mean ± S.D.

uncorrected. IR spectra were recorded on Shimadzu 8400 S FT-IR spectrophotometer using KBr pellets from 400 to 4000 cm^{-1}. Proton (^1H) Nuclear Magnetic Resonance (^1HNMR) and $^{13}CNMR$ spectra were obtained using Bruker Avance II 400 MHz and 400 MHz respectively using DMSO as a solvent. Mass spectra was recorded on Shimadzu QP2010 ULTRA GC–MS. Chemical shifts were obtained in parts per million (ppm) with tetramethylsilane (TMS) as an internal standard, and coupling constant (J) values are stated in Hertz (Hz). The following notations expressed the peak types in the spectra: singlet (s), doublet (d), triplet (t) and multiplet (m).

4.1. Chemistry

4.1.1. Synthesis of thiazolidine-2,4-dione **(3)**

A solution of chloroacetic acid (0.6 M) in 60 mL of water and thiourea (0.6 M) in 60 mL of water was stirred for 15–20 min to obtain white precipitates. To the content, 60 mL of concentrated hydrochloric acid was added. Then, the reaction mixture was refluxed for 8–10 h at 100–110 °C. On cooling, the contents were solidified into white needles as TZD **(3)** and was filtered and washed with water. The compound was then recrystallized from ethyl alcohol. The purity of synthesized compound was ascertained by TLC using ethyl acetate: hexane (80:20) as the mobile phase. Yield: 64%; IR (KBr, cm^{-1}): 1736.74 and 1671.24 (two C═O), 3482.62 (N—H), 1338.53 (C—H, bend), 3052.17 (C—H, strech), 627.85 (C—S); ^1H NMR (400 MHz, DMSO, δ ppm): 3.9 (s, 2H, CH_2), 9.8 (s, 1H, NH).

4.1.2. Synthesis of pyrazole-4-carbaldehydes **(7a-g)**

3-(4-substituted-phenyl)-1-phenyl-1H-pyrazole-4-carbaldehyde was prepared by the reaction of acetophenone and its derivatives with phenyl hydrazine in presence of ethanol as a solvent and acetic acid as catalyst, then the resulted hydrazone derivative was treated with the Vilsmeier-Haack reagent (DMF–$POCl_3$) leading to the corresponding 4-carboxaldehyde functionalized pyrazole ring **(7a-g).** The progress of the reaction was ascertained by TLC using ethyl acetate: hexane (70:30) as the mobile phase. Yield: 80%; IR (KBr, cm^{-1}): 3060.82 (aromatic C—H), 1600.98 and 1450.37 (aromatic C═C), 697.81 (aromatic C═C-H bending), 1656.63 (C═O).

4.1.3. Synthesis of N-substituted TZD **(10 and 11)**

The synthesis of *N*-benzylated TZD was carried out on stirring at 50–55 °C by taking 1.7 mmol of TZD, benzyl bromide (1.1 equivalents) and potassium carbonate (2 equivalents) in solvent DMF (4 mL). The reaction gets completed in 2–3 h and was monitored by TLC. After

Table 2
IC_{50} values obtained by alpha-amylase inhibition.

Compound Code	% Inhibition (mean ± S.D.)* (μg/mL)				IC_{50} (μg/mL)
	50	100	150	200	
GB1	52.71 ± 0.62	62.62 ± 0.22	75.56 ± 0.35	87.61 ± 0.25	41.65
GB2	−2.17 ± 0.87	4.81 ± 0.87	11.74 ± 0.87	17.88 ± 1.65	> 200
GB3	−9.31 ± 0.77	−2.21 ± 1.5	5.68 ± 1.84	13.7 ± 0.84	> 200
GB4	45.89 ± 0.21	57.82 ± 0.56	66.98 ± 0.59	78.89 ± 0.54	95.75
GB5	7.28 ± 0.98	20.21 ± 0.45	33.54 ± 0.52	47.24 ± 0.88	> 200
GB6	10.03 ± 1.5	21.43 ± 1.8	32.39 ± 0.46	45.41 ± 0.12	> 200
GB7	39.82 ± 0.21	50.21 ± 0.12	58.27 ± 0.21	69.26 ± 0.77	102.65
GB8	39.11 ± 1.6	54.21 ± 1.8	68.89 ± 0.77	83.94 ± 1.54	86.44
GB9	50.29 ± 0.14	59.97 ± 0.65	72.39 ± 0.59	82.56 ± 1.69	50.50
GB10	48.33 ± 1.8	60.39 ± 1.8	73.54 ± 0.48	85.32 ± 0.44	57.01
GB11	51.21 ± 0.8	62.71 ± 0.74	75.98 ± 0.54	86.69 ± 0.25	45.10
GB12	58.12 ± 1.9	66.31 ± 1.15	76.33 ± 0.98	85.32 ± 1.39	7.59
GB13	58.19 ± 0.26	62.09 ± 0.47	74.13 ± 1.36	87.15 ± 1.65	22.03
GB14	**58.19 ± 0.71**	**67.32 ± 1.65**	**77.01 ± 1.24**	**85.17 ± 1.58**	**4.08**
Acarbose	57.38 ± 0.25	67.99 ± 1.3	77.99 ± 0.87	85.78 ± 0.65	8.0

* Values are expressed as mean ± standard deviation (n = 3).

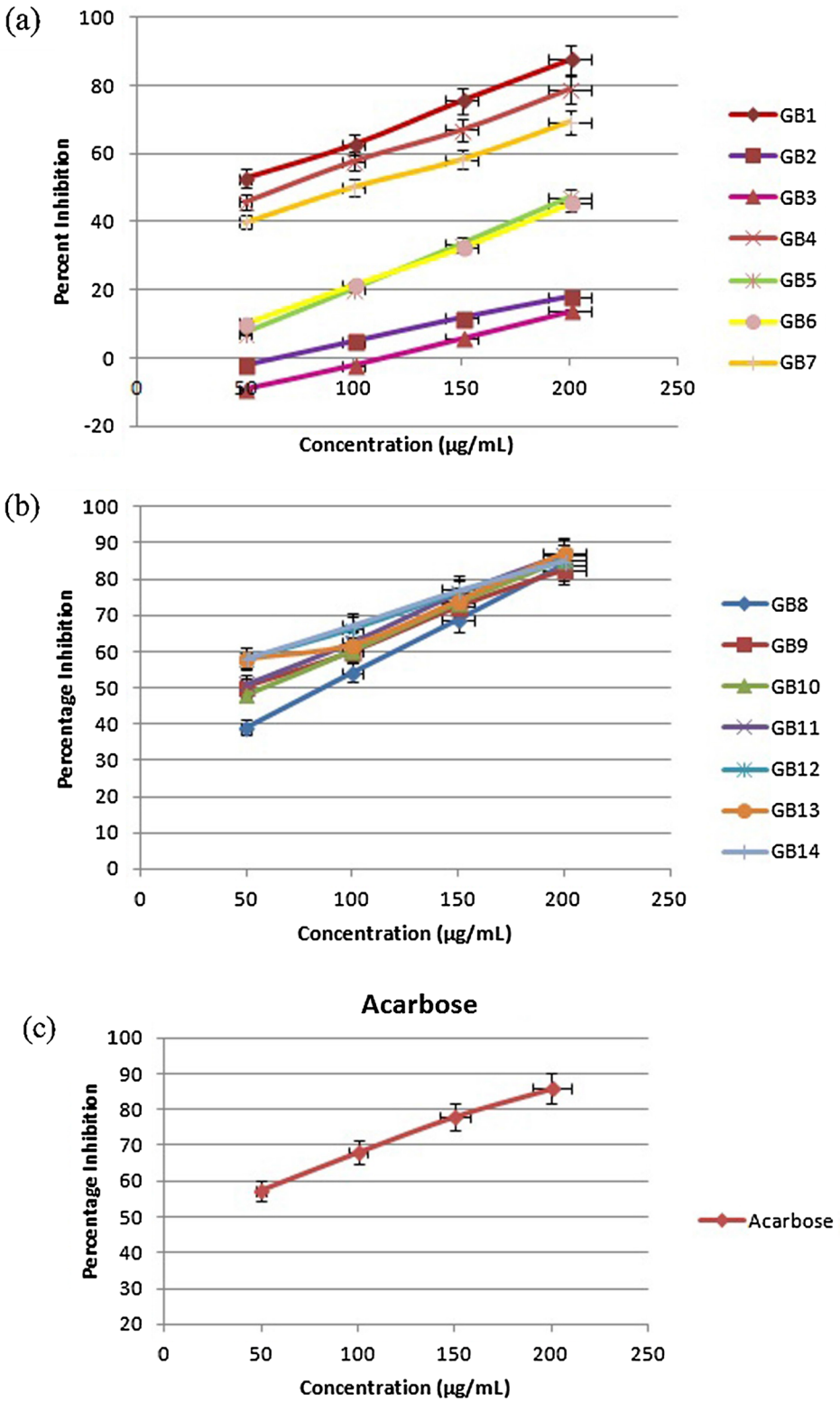

Fig. 13. (a) % inhibition of alpha-amylase enzyme by GB1-7 (b) % inhibition of alpha-amylase enzyme by GB8-14 (c) % inhibition of alpha-amylase enzyme by acarbose at different concentrations.

stirring, the reaction mixture was poured into ice cold water and the content was precipitated out and filtered and washed with cold water. Similarly, for *N*-acidic TZD, the reaction was carried out between TZD and bromoacetic acid at same reaction conditions. The products (**10** and **11**) were then recrystallised from ethanol. Yield: 85% (benzylated) and 65% (acidic); IR (KBr, cm^{-1}): 1174 (C–N), 1432 (CH_2), 1648 and 1771 (2 ring C=O), 1541 (aromatic C=C), 3058.75 (aromatic C–H), 1720 (acidic C=O), 3240 (OH stretch), 946 (OH bend).

*4.1.4. Synthesis of final derivatives (Knoevenagel condensation) **(GB1-14)***

The final step involves the Knoevenagel condensation of various pyrazole carbaldehydes with *N*-substituted TZDs (both benzylated and

Table 3
TNF-α activity of synthesized derivatives.

Compound	TNF-α activity (pg/mL)			Mean ± S.E.M.
	i	ii	iii	
Control	508	515	522	515 ± 4.04
GB1	250	257	260	255.66 ± 2.96
GB2	210	215	218	214.33 ± 2.33
GB3	218	207	212	212.33 ± 3.17
GB5	357	348	360	355 ± 6.24
GB7	**197**	**190**	**205**	**197.33 ± 4.33**
GB8	410	398	412	406.67 ± 4.37
GB9	310	302	315	309 ± 3.78
GB10	467	458	462	462.33 ± 2.60
GB11	290	282	275	282.33 ± 4.33
GB14	305	298	311	304.67 ± 3.75
Etoricoxib	183	189	187	186.33 ± 1.76

Table 4
IL-β activity of synthesized derivatives.

Compound	IL-1β activity (pg/mL)			Mean ± S.E.M.
	i	ii	iii	
Control	680	672	686	679.33 ± 4.05
GB1	22	18	26	22 ± 2.30
GB2	**15**	**22**	**12**	**16.33 ± 2.96**
GB3	28	22	19	23 ± 2.64
GB5	36	28	31	31.66 ± 2.33
GB7	24	20	17	20.33 ± 2.02
GB8	62	71	66	66.33 ± 2.60
GB9	36	29	32	32.33 ± 2.02
GB10	32	28	31	30.33 ± 1.20
GB11	51	46	55	50.66 ± 2.60
GB14	35	30	28	31 ± 2.08
Etoricoxib	16	24	23	21 ± 2.51

Table 5
MDA activity of synthesized derivatives.

Compound	MDA activity (nM/mg)			Mean ± S.E.M.
	(i)	(ii)	(iii)	
Control	22.4	23.2	23.6	23.06 ± 0.35
GB1	10.6	11.2	12	11.26 ± 0.40
GB2	9.2	10.5	9.8	9.83 ± 0.37
GB3	10.8	9.9	10.2	10.3 ± 0.26
GB5	11.4	10.5	12	11.3 ± 0.43
GB7	**4.6**	**6**	**5.5**	**5.36 ± 0.40**
GB8	19.6	17	20.2	18.93 ± 0.98
GB9	13.4	10.5	12.7	12.2 ± 0.87
GB10	14.6	12	13.2	13.26 ± 0.75
GB11	12.2	10	11.5	11.23 ± 0.64
GB14	8.4	10.2	9.5	9.36 ± 0.52
Etoricoxib	4.3	5	4.9	4.73 ± 0.21

acidic). The perfect spot was observed in TLC the product was obtained in good yield. The solvent system used for TLC is toluene: ethyl acetate: formic acid (8.0:1.5:0.5). All the title compounds GB (1–14) were obtained in satisfactory yield after purification by recrystallization.

*4.1.4.1. 3-benzyl-5-((1,3-diphenyl-1H-pyrazol-4-yl)methylene) thiazolidine-2,4-dione (**GB1**).* Yield: 85%; IR (KBr, cm^{-1}): 1739 and 1686 (two C═O), 1614 (C═N), 3067 (aromatic C−H), 1597 and 1456 (aromatic C═C), 2924 (aliphatic C−H); ^{1}H NMR (400 MHz, DMSO, δ ppm): 8.51–8.49 (1H, s, pyrazolyl H), 7.45–7.43 (1H, s, ═CH−), 4.85–4.83 (2H, s, N-CH_2), 7.82–7.23 (15H, m, aromatic H); ^{13}C NMR (400 MHz, DMSO, δ ppm): 168.04–165.37 (2C═O), 139.82–139.03 (−CH═), 155.37–154.23 (C-3 and 5, pyrazolyl ring), 44.63–44.46 (N-CH2), 119–137 (aromatic C); Mass (*m/z*): 437.51 $[M+H]^+$.

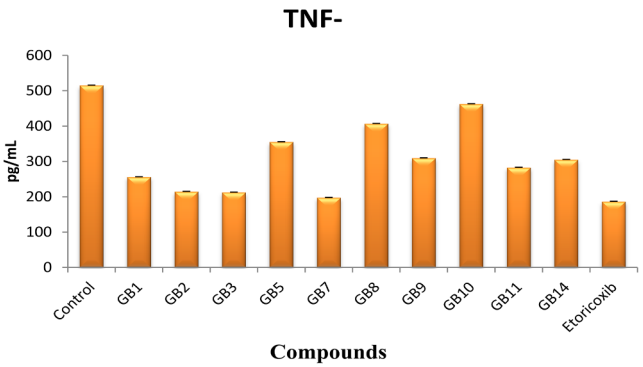

Fig. 14. TNF-α activity taken in triplicate of the synthesized compounds.

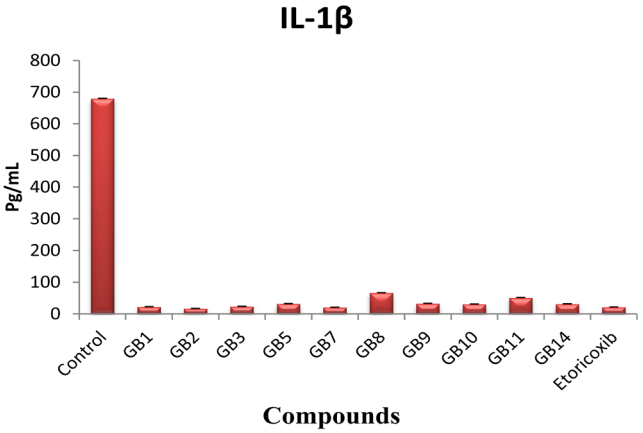

Fig. 15. IL-β activity taken in triplicate of the synthesized compounds.

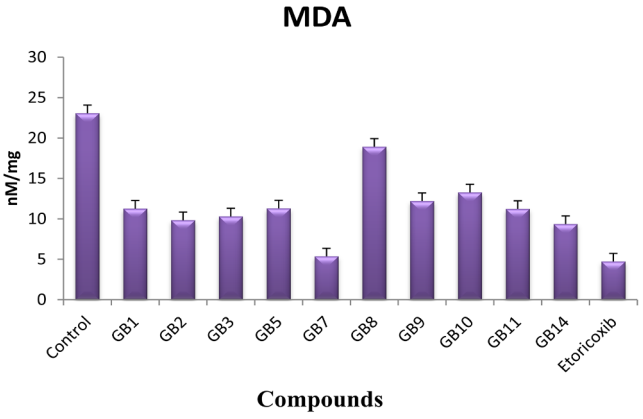

Fig. 16. MDA activity taken in triplicate of the synthesized compounds.

*4.1.4.2. 3-benzyl-5-((3-(4-fluorophenyl)-1-phenyl-1H-pyrazol-4-yl) methylene)thiazolidine-2, 4-dione (**GB2**).* Yield: 82%; IR (KBr, cm^{-1}): 1740 and 1686 (two C═O), 1613 (C═N), 3056 (aromatic C−H), 1598 and 1452 (aromatic C═C), 1598 (aliphatic C═C), 2946 (aliphatic C−H), 1243 (C-F stretch); ^{1}H NMR (400 MHz, DMSO, δ ppm): 8.81–8.79 (1H, s, pyrazolyl H), 7.73–7.71 (1H, s, ═CH−), 4.36–4.32 (2H, s, N-CH_2), 7.60–7.21 (12H, m, aromatic H), 8.04–8.02 (2H, m, aromatic H); ^{13}C NMR (400 MHz, DMSO, δ ppm): 159.30–167.77 (2C═O), 140.8–142.7 (−CH═), 151.7–154.23 (C-3 and 5, pyrazolyl ring), 44.88–44.94 (N-CH_2), 114–131 (aromatic C); Mass (*m/z*): 455.50 $[M+H]^+$.

Table 6
IC_{50} values obtained by DPPH assay.

Compound Code	% Radical scavenging activity (mean ± S.D.)				IC_{50} (μg/mL)
	50 μg/mL	100 μg/mL	150 μg/mL	200 μg/mL	
GB1	23.52 ± 0.02	37.69 ± 0.03	52.36 ± 0.03	65.67 ± 2.1	143.51
GB2	19.65 ± 0.12	33.67 ± 0.15	46.70 ± 0.05	61.69 ± 0.14	159.56
GB3	22.83 ± 0.06	35.83 ± 0.19	48.38 ± 1.6	62.33 ± 0.19	154.27
GB4	**32.97 ± 0.09**	**46.96 ± 0.09**	**61.12 ± 1.7**	**75.21 ± 2.7**	**110.88**
GB5	34.12 ± 0.13	44.18 ± 0.08	55.23 ± 2.1	64.81 ± 0.04	127.18
GB6	27.29 ± 0.15	40.26 ± 0.14	52.33 ± 0.09	60.36 ± 0.09	147.56
GB7	31.79 ± 0.04	41.29 ± 0.22	51.80 ± 0.04	61.02 ± 0.06	143.26
GB8	32.21 ± 0.12	43.66 ± 0.21	54.21 ± 0.06	66.96 ± 1.3	128.55
GB9	28.02 ± 0.21	37.17 ± 0.06	47.33 ± 0.07	55.74 ± 0.04	168.11
GB10	29.22 ± 0.013	36.14 ± 0.16	42.36 ± 1.2	51.38 ± 0.03	195.86
GB11	27.01 ± 0.09	40.06 ± 0.23	52.13 ± 0.03	61.36 ± 0.08	146.26
GB12	24.96 ± 0.06	35.42 ± 0.08	46.78 ± 0.08	58.32 ± 1.3	164.36
GB13	25.88 ± 0.04	36.86 ± 0.03	46.88 ± 1.3	58.86 ± 1.4	161.84
GB14	25.16 ± 0.01	36.66 ± 1.4	47.56 ± 2.3	57.36 ± 0.08	210.18
Ascorbic acid	43.22 ± 0.19	54.18 ± 0.09	65.13 ± 0.03	78.10 ± 0.04	81.12

*4.1.4.3. 3-benzyl-5-((3-(4-chlorophenyl)-1-phenyl-1H-pyrazol-4-yl) methylene)thiazolidine-2, 4-dione (**GB3**)*. Yield: 80%; IR (KBr, cm^{-1}): 1740 and 1686 (two C═O), 1613 (C═N), 3124 (aromatic C−H), 1598 and 1452 (aromatic C═C), 1540 (aliphatic C═C), 2946 (aliphatic C−H), 730 (C-Cl stretch), ^{1}H NMR (400 MHz, DMSO, δ ppm): 8.68 (1H, s, pyrazolyl H), 7.74 (1H, s, ═CH−), 4.84 (2H, s, N-CH_2), 7.67–7.29 (12H, m, aromatic H), 8.20–8.00 (2H, m, aromatic H); ^{13}C NMR (400 MHz, DMSO, δ ppm): 165.51 and 151.59 (2C═O), 139.15 (−CH═), 184.14 and 152.88 (C-3 and 5, pyrazolyl ring), 40.59 (N-CH_2), 115–135 (aromatic C); Mass (*m/z*): 471.96 $[M+H]^+$.

*4.1.4.4. 3-benzyl-5-((3-(4-hydroxyphenyl)-1-phenyl-1H-pyrazol-4-yl) methylene)thiazolidine- 2,4-dione (**GB4**)*. Yield: 73%; IR (KBr, cm^{-1}): 1739 and 1683 (two C═O), 1610 (C═N), 3125 (aromatic C−H), 1598 and 1446 (aromatic C═C), 1520 (aliphatic C═C), 2948 (aliphatic C−H), 3387 (OH stretch); ^{1}H NMR (400 MHz, DMSO, δ ppm): 8.70 (1H, s, pyrazolyl H), 7.72 (1H, s, ═CH−), 4.28 (2H, s, N-CH_2), 7.99–7.29 (12H, m, aromatic H), 6.95–6.90 (2H, m, aromatic H), 9.96 (1H, m, OH); ^{13}C NMR (400 MHz, DMSO, δ ppm): 167.47 and 165.74 (2C═O), 139.28 (−CH═), 154.51 and 185.17 (C-3 and 5, pyrazolyl ring), 45.16 (N-CH_2), 115.57–129.13 (aromatic C); Mass (*m/z*): 453.51 $[M+H]^+$.

*4.1.4.5. 3-benzyl-5-((3-(4-methoxyphenyl)-1-phenyl-1H-pyrazol-4-yl) methylene)thiazolidine-2,4-dione (**GB5**)*. Yield: 78%; IR (KBr, cm^{-1}): 1739 and 1685 (two C═O), 1610 (C═N), 3123 (aromatic C−H), 1577 and 1454 (aromatic C═C), 1521 (aliphatic C═C), 2932 (aliphatic C−H); ^{1}H NMR (400 MHz, DMSO, δ ppm): 8.78–8.67 (1H, s, pyrazolyl H), 7.74–7.70 (1H, s, ═CH−), 4.36–4.28 (2H, s, N-CH_2), 7.59–7.18 (12H, m, aromatic H), 8.03–8.01 (2H, m, aromatic H), 3.84–3.82 (3H, s, OCH_3); ^{13}C NMR (400 MHz, DMSO, δ ppm): 167.2 and 167.7 (2C═O), 141.3 (−CH═), 151.2 and 161.3 (C-3 and 5, pyrazolyl ring), 44.63 (N-CH_2), 115.82–129.65 (aromatic C), 56.3 (OCH_3); Mass (*m/z*): 467.54 $[M+H]^+$.

*4.1.4.6. 3-benzyl-5-((1-phenyl-3-(p-tolyl)-1H-pyrazol-4-yl)methylene) thiazolidine-2,4-dione (**GB6**)*. Yield: 69%; IR (KBr, cm^{-1}): 1740 and 1686 (two C═O), 1613 (C═N), 3121 (aromatic C−H), 1577 and 1522 (aromatic C═C), 1613 (aliphatic C═C), 2922 (aliphatic C−H); ^{1}H NMR (400 MHz, DMSO, δ ppm): 8.79–8.77 (1H, s, pyrazolyl H), 7.74–7.70 (1H, s, ═CH−), 4.34–4.31 (2H, s, N-CH_2), 7.79–7.38 (12H, m, aromatic H), 8.04–8.01 (2H, m, aromatic H), 2.40–2.38 (3H, s, CH_3); ^{13}C NMR (400 MHz, DMSO, δ ppm): 167.6 and 168.1 (2C═O), 141.6 (−CH═), 151.4 and 143.7 (C-3 and 5, pyrazolyl ring), 46.63 (N-CH_2), 114.2–132.39 (aromatic C), 21.6 (CH_3); Mass (*m/z*): 451.54 $[M+H]^+$.

*4.1.4.7. 3-benzyl-5-((3-(4-nitrophenyl)-1-phenyl-1H-pyrazol-4-yl) methylene)thiazolidine-2,4 -dione (**GB7**)*. Yield: 61%; IR (KBr, cm^{-1}): 1742 and 1686 (two C═O), 1616 (C═N), 3119 (aromatic C−H), 1599 and 1523 (aromatic C═C), 1523 (aliphatic C═C), 2922 (aliphatic C−H); ^{1}H NMR (400 MHz, DMSO, δ ppm): 8.83 (1H, s, pyrazolyl H), 7.74 (1H, s, ═CH−), 4.67 (2H, s, N-CH_2), 8.02–7.20 (12H, m, aromatic H), 8.41–8.39 (2H, m, aromatic H); ^{13}C NMR (400 MHz, DMSO, δ ppm): 165.59 and 167.35 (2C═O), 139.02 (−CH═), 150.36 and 184.81 (C-3 and 5, pyrazolyl ring), 45.24 (N-CH_2), 116.35–135.95 (aromatic C); Mass (*m/z*): 482.51 $[M+H]^+$.

*4.1.4.8. 2-(5-((1,3-diphenyl-1H-pyrazol-4-yl)methylene)-2,4-dioxothiazolidin-3-yl)acetic acid (**GB8**)*. Yield: 69%; IR (KBr, cm^{-1}): 1736 and 1671 (two C═O), 1597 (C═N), 3123 (aromatic C−H), 1518 and 1452 (aromatic C═C), 2854 (aliphatic C−H), 3449 (OH); ^{1}H NMR (400 MHz, DMSO, δ ppm): 8.80–8.78 (1H, s, pyrazolyl H), 7.69–7.67 (1H, s, ═CH−), 4.35–4.31 (2H, s, N-CH_2), 7.72–7.43 (15H, m, aromatic H), 9.99 (1H, s, COOH); ^{13}C NMR (400 MHz, DMSO, δ ppm): 167.3 and 167.6 (2C = O), 140.32 (−CH═), 148.98 and 152.36 (C-3 and 5, pyrazolyl ring), 43.71 (N-CH_2), 116.59–135.69 (aromatic C), 165.92 (COOH); Mass (*m/z*): 405.43 $[M+H]^+$.

*4.1.4.9. 2-(5-((3-(4-fluorophenyl)-1-phenyl-1H-pyrazol-4-yl)methylene)-2,4-dioxothiazolidin- 3-yl)acetic acid (**GB9**)*. Yield: 71%; IR (KBr, cm^{-1}): 1744 and 1673 (two C═O), 1596 (C═N), 3066 (aromatic C−H), 1522 and 1454 (aromatic C═C), 2837 (aliphatic C−H), 3426 (OH); ^{1}H NMR (400 MHz, DMSO, δ ppm): 8.81–8.79 (1H, s, pyrazolyl H), 7.72 (1H, s, ═CH−), 4.36–4.33 (2H, s, N-CH_2), 7.60–7.21 (12H, m, aromatic H), 8.04–8.01 (2H, m, aromatic H), 10.01 (1H, s, COOH); ^{13}C NMR (400 MHz, DMSO, δ ppm): 167.0 and 166.7 (2C = O), 141.03 (−CH═), 149.99 and 148.26 (C-3 and 5, pyrazolyl ring), 43.63 (N-CH_2), 116.96–133.54 (aromatic C), 165.39 (COOH); Mass (*m/z*): 423.42 $[M+H]^+$.

*4.1.4.10. 2-(5-((3-(4-chlorophenyl)-1-phenyl-1H-pyrazol-4-yl) methylene)-2,4-dioxothiazolidi -n-3-yl)acetic acid (**GB10**)*. Yield: 65%; IR (KBr, cm^{-1}): 1735 and 1672 (two C═O), 1599 (C═N), 3063 (aromatic C−H), 1599 and 1570 (aromatic C═C), 1522 (aliphatic C═C), 2861 (aliphatic C−H), 3472 (OH); ^{1}H NMR (400 MHz, DMSO, δ ppm): 8.28 (1H, s, pyrazolyl H), 7.97 (1H, s, ═CH−), 3.36 (2H, s, N-CH_2), 7.60–7.49 (12H, m, aromatic H), 8.02–8.00 (2H, m, aromatic H), 9.98 (1H, s, COOH); ^{13}C NMR (400 MHz, DMSO, δ ppm): 167.35 and 165.59 (2C═O), 138.98 (−CH═), 151.50 and 184.92 (C-3 and 5, pyrazolyl ring), 40.34 (N-CH_2), 119.73–136.21 (aromatic C), 166.39 (COOH); Mass (*m/z*): 439.87 $[M+H]^+$.

4.1.4.11. 2-(5-((3-(4-hydroxyphenyl)-1-phenyl-1H-pyrazol-4-yl)

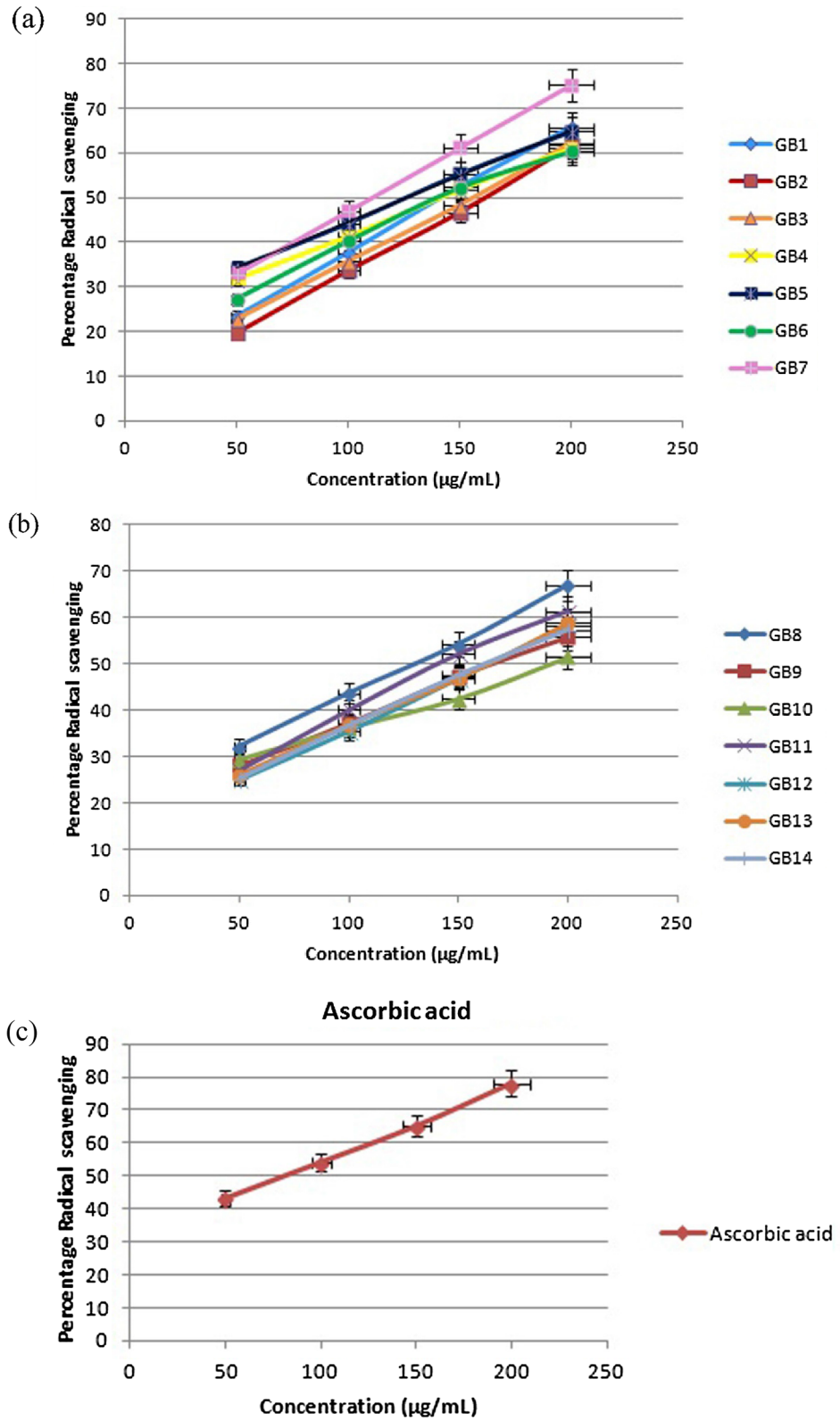

Fig. 17. (a) % of radical scavenging by GB1-7 (b) % of radical scavenging by GB8-14 (c) % of radical scavenging by ascorbic acid at different concentrations.

*methylene)-2,4-dioxothiazoli -din-3-yl)acetic acid (**GB11**)*. Yield: 70%; IR (KBr, cm^{-1}): 1735 and 1686 (two C═O), 1615 (C═N), 3109 (aromatic C–H), 1597 and 1519 (aromatic C═C), 1449 (aliphatic C═C), 2857 (aliphatic C–H), 3348 (OH); ^{1}H NMR (400 MHz, DMSO, δ ppm): 8.75 (1H, s, pyrazolyl H), 7.72 (1H, s, ═CH–), 4.36 (2H, s, N-CH_2), 7.59–7.29 (12H, m, aromatic H), 6.96–6.93 (2H, m, aromatic H), 9.88 (1H, m, OH), 10.11 (1H, s, COOH); ^{13}C NMR (400 MHz, DMSO, δ ppm): 167.4 and 167.8 (2C═O), 140.52 (–CH═), 152.26 and 156.41 (C-3 and 5, pyrazolyl ring), 43.71 (N-CH_2), 116.48–131.54 (aromatic C), 165.74 (COOH); Mass (*m/z*): 421.43 $[M + H]^+$.

*4.1.4.12. 2-(5-((3-(4-methoxyphenyl)-1-phenyl-1H-pyrazol-4-yl) methylene)-2,4-dioxothiazoli -din-3-yl)acetic acid (**GB12**).* Yield: 68%; IR (KBr, cm^{-1}): 1736 and 1676 (two C═O), 1611 (C═N), 3123 (aromatic C−H), 1600 and 1580 (aromatic C═C), 1522 (aliphatic C═C), 2933 (aliphatic C−H), 3448 (OH); ^{1}H NMR (400 MHz, DMSO, δ ppm): 8.78 (1H, s, pyrazolyl H), 7.74–7.70 (1H, s, ═CH−), 4.36–4.28 (2H, s, N-CH_2), 7.59–7.18 (12H, m, aromatic H), 8.03–8.01 (2H, m, aromatic H), 3.84–3.82 (3H, s, OCH_3), 9.98 (1H, s, COOH); ^{13}C NMR (400 MHz, DMSO, δ ppm): 167.2 and 167.5 (2C═O), 141.18 (−CH═), 147.58 and 152.3 (C-3 and 5, pyrazolyl ring), 42.98 (N-CH_2), 115.29–131.09 (aromatic C), 165.68 (COOH), 57.1 (OCH_3); Mass (*m/z*): 435.45 [M + H]$^{+}$.

*4.1.4.13. 2-(5-((3-(4-methoxyphenyl)-1-phenyl-1H-pyrazol-4-yl) methylene)-2,4-dioxothiazoli -din-3-yl)acetic acid (**GB12**).* Yield: 68%; IR (KBr, cm^{-1}): 1736 and 1676 (two C═O), 1611 (C═N), 3123 (aromatic C−H), 1600 and 1580 (aromatic C═C), 1522 (aliphatic C═C), 2933 (aliphatic C−H), 3448 (OH); ^{1}H NMR (400 MHz, DMSO, δ ppm): 8.78 (1H, s, pyrazolyl H), 7.74–7.70 (1H, s, ═CH−), 4.36–4.28 (2H, s, N-CH_2), 7.59–7.18 (12H, m, aromatic H), 8.03–8.01 (2H, m, aromatic H), 3.84–3.82 (3H, s, OCH_3), 9.98 (1H, s, COOH); ^{13}C NMR (400 MHz, DMSO, δ ppm): 167.2 and 167.5 (2C═O), 141.18 (−CH═), 147.58 and 152.3 (C-3 and 5, pyrazolyl ring), 42.98 (N-CH_2), 115.29–131.09 (aromatic C), 165.68 (COOH), 57.1 (OCH_3); Mass (*m/z*): 435.45 [M + H]$^{+}$.

*4.1.4.14. 2-(2,4-dioxo-5-((1-phenyl-3-(p-tolyl)-1H-pyrazol-4-yl) methylene)thiazolidin-3-yl)- acetic acid (**GB13**).* Yield: 62%; IR (KBr, cm^{-1}): 1734 and 1672 (two C═O), 1599 (C═N), 3123 (aromatic C−H), 1599 and 1565 (aromatic C═C), 1521 (aliphatic C═C), 2922 (aliphatic C−H), 3448 (OH); ^{1}H NMR (400 MHz, DMSO, δ ppm): 7.99 (1H, s, pyrazolyl H), 7.59 (1H, s, ═CH−), 3.83 (2H, s, N-CH_2), 7.59–7.05 (12H, m, aromatic H), 7.99 (2H, m, aromatic H), 2.51–2.50 (3H, s, CH_3), 9.97 (1H, s, COOH); ^{13}C NMR (400 MHz, DMSO, δ ppm): 166.84 and 167.5 (2C═O), 139.09 (−CH═), 160.53 and 185.04 (C-3 and 5, pyrazolyl ring), 42.98 (N-CH_2), 114.43–135.40 (aromatic C), 166.78 (COOH), 21.8 (CH_3); Mass (*m/z*): 419.45 [M + H]$^{+}$.

*4.1.4.15. 2-(5-((3-(4-nitrophenyl)-1-phenyl-1H-pyrazol-4-yl)methylene)-2,4-dioxothiazolidin − 3-yl)acetic acid (**GB14**).* Yield: 57%; IR (KBr, cm^{-1}): 1735 and 1688 (two C═O), 1637 (C═N), 3125 (aromatic C−H), 1672 and 1600 (aromatic C═C), 1523 (aliphatic C═C), 2917 (aliphatic C−H), 3448 (OH); ^{1}H NMR (400 MHz, DMSO, δ ppm): 8.88 (1H, s, pyrazolyl H), 7.76 (1H, s, ═CH−), 4.38 (2H, s, N-CH_2), 8.06–7.43 (12H, m, aromatic H), 8.43–8.40 (2H, m, aromatic H), 10.54 (1H, s, COOH); ^{13}C NMR (400 MHz, DMSO, δ ppm): 167.17 and 167.29 (2C═O), 139.04 (−CH═), 151.69 and 148.98 (C-3 and 5, pyrazolyl ring), 43.79 (N-CH_2), 116.33–130.18 (aromatic C), 165.40 (COOH); Mass (*m/z*): 450.42 [M + H]$^{+}$.

4.2. Molecular docking studies

The structure of desired targets PPAR-γ and α-amylase enzymes has been selected and extracted from Protein Data Bank (PDB: http://www.rcsb.org/pdb). The structures of internal ligands (Pioglitazone and acarbose) and final derivatives (GB-1-14) have been drawn by using Chem Draw Ultra 12.0 software. The ligands were energy minimized by selecting force field MMFF94x, Austin model 1 (AM 1) with gradient value of 0.0001 kcal/mol and were saved as mdb format. The selected protein was subjected to protein preparation in Set up wizard by using Molecular Operating Environment (MOE) version 2008.10 software. The docking simulations were predicted by docking the prepared ligands in the binding pocket of PPAR-γ and α-amylase and the results were displayed in database viewer. 2D and 3D interactions of ligands with the receptor were predicted using compute tool. The docking results were compared to the standard drug pioglitazone and acarbose for both antidiabetic and amylase inhibition activity, respectively. The Mol Dock score values were then calculated.

4.3. Biological activity

4.3.1. In vivo antidiabetic activity

Mice were housed in groups of six in clean poly acrylic cages. husk as bedding material of the cages was changed every day. The animals were maintained under natural day and night cycle. Animals were acclimatized for one week to the laboratory conditions before starting the experiment. Animals were given standard pellet diet and allowed water *ad libitum*. All the animal studies were conducted in accordance with the guidelines for animal care. The protocol was approved by the Institutional Animal Ethics Committee () (Reg. No.816/PO/ReBiBt/S/04/CPCSEA).

Male C57BL/6J mice, weighing about 23–27 gm were used for antidiabetic studies. Animals were divided into following groups consisting of six rats. Group 1: Consisted of healthy rats and received 0.5 mL of 0.9% normal saline; Group 2: diabetic rats received STZ (180 mg/kg b.w.)-NA (210 mg/kg b.w.) injection; Group 3: diabetic rats orally fed with pioglitazone (as 0.25% CMC suspension) at a dose of 10 mg/kg; Group 4–7: diabetic rats orally fed with synthesized compounds (GB-8, GB-11 and GB-14) (as 0.25% CMC suspension) at a dose of 30 mg/kg. The blood glucose level of every group was checked at 0, 1, 7, and 15 days through glucometer by withdrawing 0.1–0.2 mL of blood from tail vein under mild ether anesthesia [26].

4.3.1.1. Statistical analysis. All the values of the experimental results were expressed as mean ± SD and analyzed by one-way analysis of variance (ANOVA, Dunnett's test) for the possible significant identification between various groups. $P < 0.001$ was considered statistically significant. Statistical analysis was carried out using Graph pad prism 3.0 (Graph pad software, San Diego, CA).

4.3.2. In vitro alpha-amylase activity

In humans, the digestion of starch involves several stages. Initially, partial digestion by the salivary amylase results in the degradation of polymeric substrates into shorter oligomers. Later on in the gut these are further hydrolyzed by pancreatic α-amylases into maltose, maltotriose and small malto-oligosaccharides. The digestive enzyme (α-amylase) is responsible for hydrolyzing dietary starch (maltose), which breaks down into glucose prior to absorption. Inhibition of α-amylase can lead to reduction in post prandial hyperglycemia in diabetic condition [27].

4.3.2.1. Principle. Alpha-amylase activity can be measured *in vitro* by hydrolysis of starch in presence of α-amylase enzyme. This process was quantified by using iodine, which gives blue color with starch. The reduced intensity of blue colour indicates the enzyme-induced hydrolysis of starch in to monosaccharides. If the substance/extract possesses α-amylase inhibitory activity, the intensity of blue colour will be more. In other words, the intensity of blue color in test sample is directly proportional to α-amylase inhibitory activity [28].

4.3.2.2. Procedure

1. Preparation of phosphate buffer (0.02 M, pH = 6.9)

Solutions of 0.02 M of $Na_2HPO_4{\cdot}12H_2O$ and $NaH_2PO_4{\cdot}H_2O$ were prepared separately and their pH was detected by pH meter, thereafter the solution with lower pH ($NaH_2PO_4{\cdot}H_2O$) was poured into solution with higher pH ($Na_2HPO_4{\cdot}_{12}H_2O$) and rechecked pH of the solution again, and adjusted by drop-wise addition of 0.006 M NaCl or 1% NaOH solution to 6.9.

2. Preparation of (0.5 mg/mL) alpha-amylase solution

12.5 mg of aspergillus alpha-amylase was dissolved in minimum quantity of prepared phosphate buffer (pH 6.9) in a 25 mL volumetric flask, thereafter complete solubility; volume was made up to 25 mL by the same solution.

3. Preparation of 1% starch solution

1 g of potato starch was dissolved in 100 mL of distilled water and boiled for 30 s on a hot plate. The solution was cooled at room and filtered through simple filter paper. Filtrates were used for the alpha amylase inhibitory assay.

4. Preparation of 1% iodine solution

1 g of iodine and 2 g of KI were dissolved in 50 mL of distilled water in a baker and stirred on a magnetic stirrer overnight for complete solubility of I2, thereafter solution was transferred to a 100 mL volumetric flask and volume was made up to 100 mL by the same solvent and used for the assay.

5. Preparation of stock sample solution

10 mg of each compound was dissolved in 10 mL DMSO in a volumetric flask and was labeled as a stock sample solution 1000 ppm. From a solution of stock (1000 ppm), 0.5 mL, 1 mL, 1.5 mL, and 2 mL were transferred to separate 10 mL volumetric flasks and volumes were made up by DMSO, thereafter labeled as working sample solutions 50 ppm, 100 ppm, 150 ppm, and 200 ppm. Same as working solution for standard, acarbose was made.

Alpha-amylase activity was carried out by starch-iodine method. 10 μL of α-amylase solution was mixed with 390 μL of phosphate buffer containing different concentration of extracts. After incubation at 37 °C for 10 min, 100 μL of starch solution (1%) was added, and the mixture was re-incubated for 1 h. Next, 0.1 mL of 1% iodine solution was added, and after adding 5 mL distilled water, the absorbance was taken at 565 nm. Sample, substrate and α-amylase blank determinations were carried out under the same reaction conditions [20].

4.3.2.3. Statistical analysis. The absorbance of the final reaction mixture of three parallel experiments was taken and is expressed as mean ± standard deviation. The activities were also determined as a function of their percent inhibition which was calculated by using the formula:

$$\text{Enzyme activity} = (A - B)/\ A \times 100$$

where

A = absorbance of positive control (α-amylase)
B = absorbance of sample (GB 1–14)

4.3.3. In vitro anti-inflammatory activity

4.3.3.1. Estimation of TNF-α. The TNF-α level was estimated by using rat TNF-α kit (KRISHGEN Bio System, Ashley Ct, Whittier, CA). It is a solid phase sandwich enzyme-linked immunosorbent assay (ELISA), which uses a microtitre plate reader to read at 450 nm [29].

4.3.3.1.1. Assay procedure. The reagent and standard dilutions were prepared as suggested by the manufacturer's instructions. 100 μL of standard and sample was added per well and were mixed gently. The plate was covered with the adhesive strip and incubated for 2.5 h at room temperature. Each well was then aspirated and washed with wash buffer, repeating the process four times for a total of five washes. The plate was then inverted and blotted against a clean paper towel. 100 μL of antibody was added to each well and covered with a new adhesive strip. The plate was again incubated for 2 h at room temperature with gentle shaking. Repeat the aspiration/washing. 100 μL of streptavidin solution was then added to each well and incubated for 20 min at room temperature protected from light. Discard the solution. 100 μL of TMB one-step substrate reagent was added to each well and incubated for 15 min at room temperature.100 μL of stop solution was finally added to each well and the absorbance of each well was read in an ELISA reader set to 450 nm within 30 min.

4.3.3.1.2. Statistical analysis. The average for the triplicate readings was calculated for each sample along with their standard error of mean. A graph was constructed by plotting the mean absorbance for each standard on the y-axis for different samples at particular concentration.

4.3.3.2. Estimation of IL-β. The IL-1β level was estimated by using rat IL-1β kit (KRISHGEN BioSystem, Ashley Ct, Whittier, CA). It is a solid phase sandwich enzyme-linked immunosorbent assay (ELISA), which uses a microtitre plate reader read at 450 nm. Concentrations of IL-1β were calculated from the plotted standard curve [29].

4.3.3.2.1. Assay procedure. The reagent and standard dilutions were prepared as suggested by the manufacturer's instructions. 100 μL of standard and sample was added per well and were mixed gently. The plate was covered with the adhesive strip and incubated for 2.5 h at room temperature. Each well was then aspirated and washed with wash buffer, repeating the process four times for a total of five washes. The plate was then inverted and blotted against a clean paper towel.100 μL of antibody was added to each well and covered with a new adhesive strip. The plate was again incubated for 2 h at room temperature with gentle shaking. Repeat the aspiration/washing. 100 μL of streptavidin solution was then added to each well and incubated for 20 min at room temperature protected from light. Discard the solution. 100 μL of TMB one-step substrate reagent was added to each well and incubated for 15 min at room temperature.100 μL of stop solution was finally added to each well and the absorbance of each well was read in an ELISA reader set to 450 nm within 30 min.

4.3.3.2.2. Statistical analysis. The average for the triplicate readings was calculated for each sample along with their standard error of mean. A graph was constructed by plotting the mean absorbance for each standard on the y-axis for different samples at particular concentration.

4.3.4. Antioxidant activity

The synthesized compounds were evaluated for *in vitro* antioxidant activity by DPPH (1,1-diphenyl-2-picrylhydrazyl) method using ascorbic acid as standard.

4.3.4.1. Principle. This assay is based on the theory that a hydrogen donor is an antioxidant. It measures compound that are radical scavengers. The antioxidant effect is proportional to the disappearance of DPPH in the test samples. DPPH shows a strong absorption maximum at 517 nm (purple). The color turns from purple to yellow followed by formation of DPPH upon absorption of hydrogen from an antioxidant. This reaction is stoichiometric with respect to the number of hydrogen atoms absorbed. Therefore, the antioxidant effect can be easily evaluated by following the decrease of UV absorption at 517 nm [30].

4.3.4.2. Procedure

1. Preparation of DPPH solution

0.1 mM solution of DPPH was freshly prepared in methanol and was kept in dark for 2 h.

2. Preparation of sample

10 mg of each compound was dissolved in 10 mL DMSO in a volumetric flask and was labeled as a stock sample solution 1000 ppm. From a solution of stock (1000 ppm), 0.5 mL, 1 mL, 1.5 mL, and 2 mL were

transferred to separate 10 mL volumetric flasks and volumes were made up of DMSO, thereafter labeled as working sample solutions 50 ppm, 100 ppm, 150 ppm, and 200 ppm.

2 mL of different concentrations of test samples were taken in a set of test tubes and to this, 2 mL of freshly prepared DPPH solution was added and mixed thoroughly. This final solution is then incubated for 30 min at room temperature and the absorbance was recorded at 517 nm94.

4.3.4.3. Statistical analysis. The absorbance of the final reaction mixture of three parallel experiments was taken and is expressed as mean ± standard deviation. The activities were also determined as a percentage of scavenging which was calculated by using the formula:

$$\%\,\text{Scavenging} = (A - B)/\,A \times 100$$

where

A = absorbance of control (DPPH)
B = absorbance of sample (GB 1–14).

Acknowledgements

Authors would like to acknowledge ISF College of Pharmacy, Moga for providing necessary facilities during research. The authors also acknowledge ISF Analytical Lab, Moga and Panjab University, Chandigarh for providing the sophisticated analytical instrumental facilities.

Appendix A. Supplementary material

Supplementary data to this article can be found online at https://doi.org/10.1016/j.bioorg.2019.103271.

References

[1] Diabetes is Indias fastest growing disease: 72 million cases recorded in 2017, figure expected to nearly double by 2025. < https://www.firstpost.com/india/diabetes-is-indias-fastest-growing-disease-72-million-cases-recorded-in-2017-figure-expected-to-nearly-double-by-2025-4435203.html > (accessed 02 June 2019).
[2] K.G.M.M. Alberti, P.F. Zimmet, Definition, diagnosis and classification of diabetes mellitus and its complications. Part 1: diagnosis and classification of diabetes mellitus. Provisional report of a WHO consultation, Diabetic Med. 15 (1998) 539–553, https://doi.org/10.1002/(SICI)1096-9136(199807)15:7<539::AID-DIA668>3.0.CO;2-S.
[3] H. Hauner, The mode of action of thiazolidinediones, Diab. Metab. Res. Rev. 18 (2002) S10–S15, https://doi.org/10.1002/dmrr.249.
[4] M. Brownlee, Biochemistry and molecular cell biology of diabetic complications, Nature 414 (2001) 813–820, https://doi.org/10.1038/414813a.
[5] F.N. Ziyadeh, G. Wolf, Pathogenesis of the podocytopathy and proteinuria in diabetic glomerulopathy, Curr. Diab. Rev. 4 (2008) 39–45, https://doi.org/10.2174/157339908 783502370.
[6] K.H. Jeong, T.W. Lee, C.G. Ihm, S.H. Lee, J.Y. Moon, S.J. Lim, Effects of sildenafil on oxidative and inflammatory injuries of the kidney in streptozotocin-induced diabetic rats, Am. J. Nephrol. 29 (2009) 274–282, https://doi.org/10.1159/000158635.
[7] I.M. Shah, S.P. Mackay, G.A. McKay, Therapeutic strategies in the treatment of diabetic nephropathy-a translational medicine approach, Curr. Med. Chem. 16 (2009) 997–1016, https://doi.org/10.2174/092986709787581897.
[8] R.A. Daynes, D.C. Jones, Emerging roles of PPARs in inflammation and immunity, Nat. Rev. Immunol. 2 (2002) 748–756, https://doi.org/10.1038/nri912.
[9] A.P. Rolo, C.M. Palmeira, Diabetes and mitochondrial function: role of hyperglycemia and oxidative stress, Toxicol. Appl. Pharmacol. 212 (2006) 167–178, https://doi.org/10.1016/J.TAAP.2006.01.003.
[10] N. Bashan, J. Kovsan, I. Kachko, H. Ovadia, A. Rudich, Positive and negative regulation of insulin signaling by reactive oxygen and nitrogen species, Physiol. Rev. 89 (2009) 27–71, https://doi.org/10.1152/physrev.00014.2008.
[11] D.W. Laight, M.J. Carrier, E.E. Änggård, Antioxidants, diabetes and endothelial dysfunction, Cardiovasc. Res. 47 (2000) 457–464, https://doi.org/10.1016/S0008-6363(00) 00054-7.
[12] S.U. Hossain, S. Bhattacharya, Synthesis of O-prenylated and O-geranylated derivatives of 5-benzylidene2, 4-thiazolidinediones and evaluation of their free radical scavenging activity as well as effect on some phase II antioxidant/detoxifying enzymes, Bioorg. Med. Chem. Lett. 17 (2007) 1149–1154, https://doi.org/10.1016/j.bmcl. 2006.12.040.
[13] S.S. Chung, M. Kim, B.S. Youn, N.S. Lee, J.W. Park, I.K. Lee, et al., Glutathione peroxidase 3 mediates the antioxidant effect of peroxisome proliferator-activated receptor γ in human skeletal muscle cells, Mol. Cell Biol. 29 (2009) 20–30, https://doi.org/10.1128/MCB.00544-08.
[14] R.A. DeFronzo, D. Tripathy, D.C. Schwenke, M. Banerji, G.A. Bray, T.A. Buchanan, et al., Pioglitazone for diabetes prevention in impaired glucose tolerance, N. Engl. J. Med. 364 (2011) 1104–1115, https://doi.org/10.1056/NEJMoa1010949.
[15] Y. Kanda, M. Shimoda, S. Hamamoto, K. Tawaramoto, F. Kawasaki, M. Hashiramoto, et al., Molecular mechanism by which pioglitazone preserves pancreatic β-cells in obese diabetic mice: evidence for acute and chronic actions as a PPARγ agonist, Am. J. Physiol. Endocrinol. Metab. 298 (2009) E278–E286, https://doi.org/10.1152/ajpendo.00388.2009.
[16] S.M. Abaraviciene, I. Lundquist, J. Galvanovskis, E. Flodgren, B. Olde, A. Salehi, Palmitate-induced β-cell dysfunction is associated with excessive NO production and is reversed by thiazolidinedione-mediated inhibition of GPR40 transduction mechanisms, PLoS One 3 (2008) e2182, , https://doi.org/10.1371/journal.pone.0002182.
[17] M. Taha, N.H. Ismail, W. Jamil, S. Imran, F. Rahim, S.M. Kashif, et al., Synthesis of 2-(2-methoxyphenyl)-5-phenyl-1,3,4-oxadiazole derivatives and evaluation of their antiglycation potential, Med. Chem. Res. 25 (2016) 225–234, https://doi.org/10.1007/s 00044-015-1476-8.
[18] R. Bashary, G.L. Khatik, Design, and facile synthesis of 1, 3 diaryl-3-(arylamino) propan-1-one derivatives as the potential alpha-amylase inhibitors and antioxidants, Bioorg. Chem. 82 (2019) 156–162, https://doi.org/10.1016/J.BIOORG.2018.10.010.
[19] G. Mishra, N. Sachan, P. Chawla, Synthesis and evaluation of thiazolidinedione-coumarin adducts as antidiabetic, anti-inflammatory and antioxidant agents, Lett. Org. Chem. 12 (2015) 429–455.
[20] A.R. Srivastava, R. Bhatia, P. Chawla, Synthesis, biological evaluation and molecular docking studies of novel 3, 5-disubstituted 2, 4-thiazolidinediones derivatives, Bioorg. Chem. 102993 (2019), https://doi.org/10.1016/j.bioorg.2019.102993.
[21] B.A. Bhat, S. Ponnala, D.P. Sahu, P. Tiwari, B.K. Tripathi, A.K. Srivastava, Synthesis and antihyperglycemic activity profiles of novel thiazolidinedione derivatives, Bioorg. Med. Chem. 12 (2004) 5857–5864, https://doi.org/10.1016/J.BMC.2004.08.031.
[22] S.N.C. Sridhar, D. Bhurta, D. Kantiwal, G. George, V. Monga, A.T. Paul, Design, synthesis, biological evaluation and molecular modelling studies of novel diaryl substituted pyrazolyl thiazolidinediones as potent pancreatic lipase inhibitors, Bioorg. Med. Chem. Lett. 27 (2017) 3749–3754, https://doi.org/10.1016/j.bmcl.2017.06.069.
[23] O. Bozdağ-Dündar, E.J. Verspohl, N. Daş-Evcimen, R.M. Kaup, K. Bauer, M. Sarıkaya, et al., Synthesis and biological activity of some new flavonyl-2, 4-thiazolidinediones, Bioorg. Med. Chem. 16 (2008) 6747–6751, https://doi.org/10.1016/j.bmc.2008.05.059.
[24] R.H. Mourão, T.G. Silva, A.L.M. Soares, E.S. Vieira, J.N. Santos, M.C.A. Lima, et al., Synthesis and biological activity of novel acridinylidene and benzylidene thiazolidinediones, Eur. J. Med. Chem. 40 (2005) 1129–1133, https://doi.org/10.1016/j.ejmech.2005.06.002.
[25] P.A. Datar, S.B. Aher, Design and synthesis of novel thiazolidine-2,4-diones as hypoglycemic agents, J. Saudi Chem. Soc. 20 (2016) S196–S201, https://doi.org/10.1016/J.J SCS.2012.10.010.
[26] M. Novelli, D. Canistro, M. Martano, N. Funel, A. Sapone, S. Melega, et al., Antidiabetic properties of a non-conventional radical scavenger, as compared to pioglitazone and exendin-4, in streptozotocin-nicotinamide diabetic mice, Eur. J. Pharmacol. 729 (2014) 37–44, https://doi.org/10.1016/j.ejphar.2014.01.071.
[27] N. Pantidos, A. Boath, V. Lund, S. Conner, G.J. McDougall, Phenolic-rich extracts from the edible seaweed, ascophyllum nodosum, inhibit α-amylase and α-glucosidase: potential anti-hyperglycemic effects, J. Funct Foods 10 (2014) 201–209, https://doi.org/10.1016/j.jff.2014.06.018.
[28] S.S. Nair, V. Kavrekar, A. Mishra, In vitro studies on alpha amylase and alpha glucosidase inhibitory activities of selected plant extracts, Euro J. Exp. Bio. 3 (2013) 128–132.
[29] N. Kaur, S. Jamwal, R. Deshmukh, V. Gauttam, P. Kumar, Beneficial effect of rice bran extract against 3-nitropropionic acid induced experimental Huntington's disease in rats, Toxicol. Rep. 2 (2015) 1222–1232, https://doi.org/10.1016/j.toxrep.2015. 08.004.
[30] M.J. Lewis, Natural product screening: anti-oxidant screen for extracts, 2012.